1966

Lateral distribution of static loads in a prestressed concrete box-beam bridge - drehersville bridge, August 1966

W. J. Douglas

D. A. VanHorn

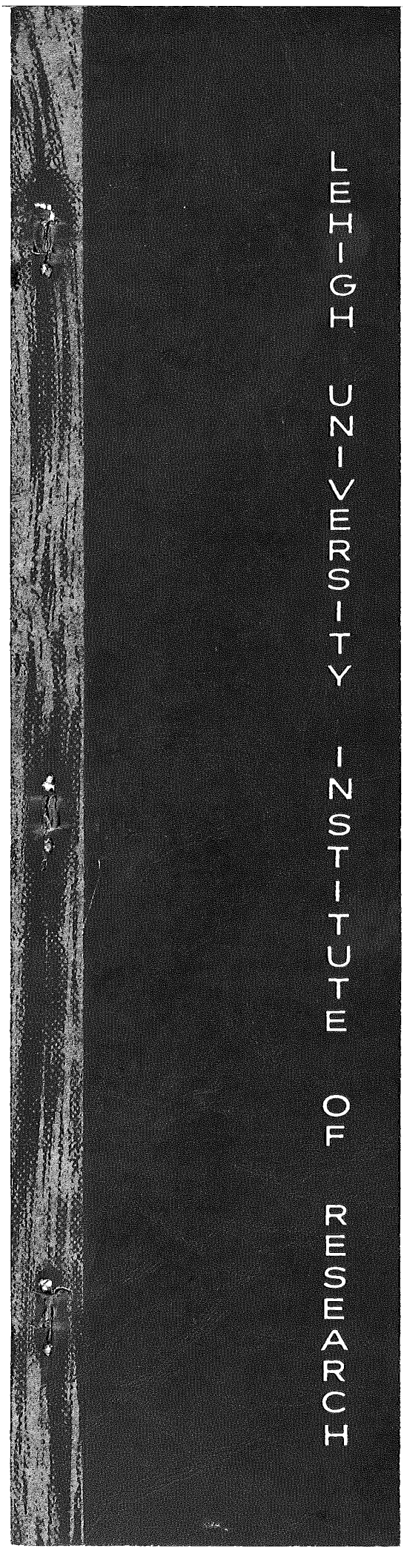

Prestressed Concrete Box-Beam Bridges
Progress Report No. 1

LATERAL DISTRIBUTION OF STATIC LOADS IN A PRESTRESSED CONCRETE BOX-BEAM BRIDGE

DREHERSVILLE BRIDGE

by
Walter J. Douglas
David A. VanHorn

Fritz Engineering Laboratory Report No. 315.1

PRESTRESSED CONCRETE BOX-BEAM BRIDGES

PROGRESS REPORT NO. 1

LATERAL DISTRIBUTION OF STATIC LOADS IN A PRESTRESSED CONCRETE BOX-BEAM BRIDGE

DREHERSVILLE BRIDGE

Walter J. Douglas
David A. VanHorn

Part of an Investigation Sponsored by:

PENNSYLVANIA DEPARTMENT OF HIGHWAYS
U. S. DEPARTMENT OF COMMERCE
BUREAU OF PUBLIC ROADS
REINFORCED CONCRETE RESEARCH COUNCIL

Fritz Engineering Laboratory
Department of Civil Engineering
Lehigh University
Bethlehem, Pennsylvania

August 1966

Fritz Engineering Laboratory Report No. 315.1

TABLE OF CONTENTS

A B S T R A C T

This report describes the field testing of the first of five beam-slab highway bridges included in an investigation of the structural behavior of bridges supported with prestressed concrete box girders, and subjected to loading with test vehicles approximating AASHO H20-S16-44 loading. The test structure was one of the end spans of a three-span simply supported bridge with a cast-in-place concrete deck supported by five precast prestressed concrete box girders laterally spaced at 7 ft. 2 in. The test span was 61 ft. 6 in. in length. The testing program consisted of the continuous recording of girder deflections and surface strains at various locations on the girders, slab, curb, and parapet, as either one or two of the test vehicles were driven over the test span at a speed of approximately 2 mph.

The principal objectives were to develop information on the distribution of vehicle loads to the girders, and to evaluate various field test techniques for use in the following studies. The measured strains were used to determine distribution factors at a cross-section near midspan. It was found that the distribution factors derived from the field measurements were substantially different from those used in the design. The test results indicated that full composite action was developed between the bridge deck, curb, and parapet. It was found that the results of superimposed single-vehicle runs closely corresponded to the results obtained from two-vehicle runs. Also, it was determined that tests on a partially gaged

cross-section could be combined to simulated tests on a fully gaged section.

This report covers test runs at crawl speeds. In addition, runs were conducted at speeds up to 34 mph. The results of the tests involving speed runs will be included in a second report.

1. INTRODUCTION

1.1 BACKGROUND

Ever since the construction of the first prestressed concrete bridge in the United States in 1950, the Walnut Lane Bridge in Philadelphia, there has been much development in the technology related to prestressed concrete bridge construction. One of these developments was the design of girder and slab bridges utilizing precast, prestressed concrete girders, along with a cast-in-place concrete slab.

Over the past few years, the Pennsylvania Department of Highways has been developing bridge designs incorporating the prestressed concrete box girder. Initially, the box shape was utilized in the construction of the adjacent box girder bridge. Lateral post-tensioning and shear keys between the adjacent girders aided in the lateral distribution of vehicle loads to the several girders composing a section. A wearing surface was applied directly to the top of the girders to serve as the deck. A later development of this initial design approach was the cast-in-place reinforced concrete slab. The slab, acting compositely with the girders, replaced lateral post-tensioning and shear keys as a method of lateral load transfer. The latest design is the spread box girder bridge, in which the girders are equally spaced and spread apart to act as T-beams with the cast-in-place slab.

1.2 OBJECT AND SCOPE

The current procedures utilized by the Pennsylvania Department of Highways in the design of prestressed concrete bridges are set forth in the PDH Bridge Division Standards ST-200 through ST-208.[11] In these standards, the interior girders of the prestressed concrete box girder beams have been proportioned according to a live load distribution factor of S/5.5 where S is the average girder spacing. This factor is identical to the factor given in the AASHO Specifications,[1] Section 3, governing the design of a concrete slab laterally continuous over interior steel I-Beam stringers. For the exterior girder, the live load is also distributed according to the general procedure set forth in the AASHO Specifications. This procedure is based on the assumption that the slab acts as a simple span between girders in transmitting wheel loads laterally.

These design procedures were instituted since it was obvious that the earlier criteria developed for the design of the adjacent box girders was not applicable to the design of the spread box girder bridges. Consequently, the procedures for live load distribution were based on a conservative estimate of the expected distribution based on the provisions governing the various members covered by the AASHO Specifications.

In 1964, the Structural Concrete Division of the Department of Civil Engineering at Lehigh University initiated an investigation of the actual load distribution characteristics for this type of bridge. The results of the study are to be compared with current

design practice, and a design procedure reflecting actual behavior is to be developed.

The overall investigation has been divided into several phases. The first phase was the field test of an existing bridge, located near Drehersville, Pennsylvania. This phase was (1) to serve as pilot test for additional field tests, and (2) to provide experimental data for use in developing a method of analysis for use in design. This report will cover the response of the Drehersville test structure to crawl-run loading. This type of loading is explained in Chapter 2. A second report will cover the behavior of the Drehersville structure under speed-run loading.

The principal objectives of this first phase were (1) to determine the actual live load distribution factors for both exterior and interior girders, and (2) to compare loading techniques, gaging patterns, and interpretation of data in evaluating experimental results. Other aspects of the study were a comparison of experimentally determined bending moments with those used in the design of the girders, the determination of girder deflections, and the study of the behavior of bridge deck, curb, and parapet in resisting applied vehicle loads.

Field testing was conducted with the Bureau of Public Roads field test unit, consisting of a loading truck and monitoring trailer. To supplement this equipment, an additional truck was provided. Test runs across the bridge were made by directing a crawling truck along one of several lanes, approximately equally spaced

across the width of the deck. The centerline of each of these lanes corresponded either to the centerline of a girder or to a line midway between girder centerlines. Data was obtained from gages located at two lateral sections. One section was located to measure maximum moment response, and the other was located to measure response with only the rear axle of the truck on the span. In addition to test runs conducted with single test trucks, simultaneous runs were made with both of the trucks side-by-side.

1.3 PREVIOUS RESEARCH

A number of field studies have been conducted on bridges constructed of concrete slabs supported by I-shaped girders, either of steel or prestressed concrete. Since the end of World War II, testing procedures have become more sophisticated, especially in the areas of measuring and recording structural response. In field tests conducted by Hindman and Vandegrift[6] in Ohio in 1945, a study of load distribution was based entirely on measured girder deflections. Test loading was achieved by the upward thrust of a hydraulic jack applied to one girder at a time. A 1952 report by Foster[5] on field studies conducted in Michigan describes the use of SR-4 strain gages on the main girder flanges, and on small cantilever beams used to measure deflections. Static strain gage measurements were obtained with a portable indicator, while dynamic measurements were permanently recorded on photo sensitive oscillograph paper. Rather than a single concentrated loading, a test truck, along with a simulated truck loaded to approximately H20-S16-44 specifications, were used.

In 1956, Holcomb[7] reported a series of field tests conducted on two bridges in Iowa. In this study, a 48-channel automatic strain recording device was utilized for both static and dynamic runs. Strains were measured on the web as well as the girder flanges. Deflections were measured by dial gages. The test vehicle, a semi-trailer totaling 98,000 lbs., did not simulate AASHO truck loading. A 1957 report by White and Purnell[15] described the field test of a composite haunched girder bridge in Texas. One of the important features of this test was the location of SR-4 strain gages on the girder in order to determine the position of the neutral axis.

The ease and speed with which field measurements can be made and recorded was improved with the Bureau of Public Roads field test equipment trailer, which houses automatic recording equipment. This trailer was first used in 1953. A tabulation by Varney and Galambos[14] of field tests conducted between 1949 and 1965 includes many studies which have utilized the BPR recording equipment. Studies of the dynamic response of a bridge in Iowa were reported in 1958 by Prentzas,[12] and describe 36-channel simultaneous recording equipment used in the testing of two bridges. In these tests, strain gages were mounted on both the top and bottom flanges of the steel girders. In 1964, dynamic tests by Reilly, Guardia and Looney[13] in Maryland report the expansion of the BPR equipment to 48-channel capacity, with the addition of a truck simulating H20-S16-44 loading. A comparable testing procedure was reported the same year for dynamic studies conducted in Virginia.[9]

Several recent tests have been conducted on I-shaped prestressed concrete girder spans. Hulsbos and Linger[8,10] reported a series of Iowa field tests of bridges, including one constructed of five prestressed concrete girders. Static loading was conducted with the test vehicle crawling across the span instead of being parked on the span. An extensive pattern of five gages was positioned on the face of a girder for experimental neutral axis determination. The Maryland tests,[13] mentioned above, included extensive testing of a nine girder prestressed concrete span.

The testing procedures used in previous field work, especially those utilized by Hulsbos and Linger,[10] aided in the planning of the field tests included in the current investigation at Lehigh University. The gaging, recording, and loading procedures were adopted from the many recent tests described in the compilation by Varney and Galambos.[14]

2. TESTING

2.1 TEST BRIDGE

The final selection of a bridge for the pilot study necessitated the meeting of several structural and site requirements. The structural requirements were that the simply supported span be of medium length, 60 to 70 feet. This span range is typical of the spread box girder bridges built in Pennsylvania. The girders were to be at right angles with the piers and abutments, with minimum superelevation of the roadway. To allow for maximum speed runs, minimum grade and tangent roadway were required. The site requirements principally involved the access to a nearby power supply, and the existence of a space which would permit parking of the instrument trailer near to the test span.

The structure which most closely conformed to the above requirements was the northwest span of the three-span bridge illustrated in Fig. 1. This bridge spans the Little Schuylkill River near Drehersville, Pennsylvania, and is located on Legislative Route 53081-1. The test span was simply supported with a length of 61 feet 6 inches. The skew was 90°, and the bridge deck was on a maximum grade of 0.2%, with normal crown. The southeast approach was on a superelevated curve, and sloped downward toward the river, allowing speed runs up to 34 mph. From the northwest, the approach was steep and short, and crossed over a single railroad track approximately 100 feet from the northwest abutment of the bridge. Therefore,

eastward speed runs were severely restricted.

The cross-section of the bridge, along with the girder designation, is shown in Fig. 2. The five identical prestressed hollow box girders, which are 48 inches wide and 33 inches deep, are equally spaced at 86 inches, center-to-center. Cast-in-place concrete diaphragms, 10 inches in thickness, are located between the beams at the ends of the span and at midspan. The reinforced concrete deck, providing a roadway 30 feet in width, was cast-in-place compositely with the girders. The specified minimum thickness of the slab was 7-1/2 inches. However, measurements taken near midspan indicate that the slab thickness actually varies from 6.2 to 7.6 inches, with an average of 6.7 inches. The safety curb, which is indicated in Fig. 2 above the lower dashed line, is composed of a 15-in. wide parapet on top of a 33-in. wide curb section. The joint between the slab and the curb was a construction joint with a raked finish. Vertical reinforcement for the curb section extended through the joint into the slab. Basically, the reinforcement consisted of three No. 5 bars laterally positioned across the joint, at a longitudinal spacing of 15 inches. For typical details of the joint, as well as other typical details of the bridge structure, see the PDH Bridge Division Standards for prestressed concrete bridges.[11]

In the design of the bridge the girders were basically proportioned for AASHO H20-S16-44 loading. For the interior girders, a distribution factor of S/5.5 = 1.302 was used, as compared to the factor of 0.814 used for the exterior girders. The impact factor

was 0.268. The specified minimum 28-day cylinder strength of the girder concete was 6000 psi; however, test cylinders indicated an average 7020 psi for the five girders. All of the girders were pre-tensioned with 46 7/16-in. seven-wire strands.

2.2 GAGE SECTIONS AND LOCATIONS

Two lateral cross-sections were selected for strain gage application. These cross-sections, specified as Sections M and N, are designated on the elevation view of the bridge, Fig. 1. Section M was located 3.55 feet west of midspan in order that maximum girder moments would be produced as the test vehicle drive axle passed over this section when proceeding westward. Section N was located 12.50 feet west of midspan. When the test truck proceeded westward, measurements could be made as the rear axle of the vehicle passed over this section, to study the effect of a single axle loading on the span.

Two gage configurations were used during field testing. The first configuration included gages at both Sections M and N. At Section M, Girders C, D, and E were gaged as shown in Fig. 3a, with two additional check gages per girder, on the bottoms of Girders A and B, for comparison with strains on Girders E and D. Five additional gages were applied at Section M, three on top of the slab above Girders C, D, and E, and two on the bottom of the slab midway between Girders C, D, and E. At Section N, Girders C, D, and E were gaged according to Fig. 3b, with two check gages on

Girders A and B, as at Section M.

For the second gage configuration, only Section M was gaged. All five girders were gaged as illustrated in Fig. 3a. Additional gaging at Section M consisted of three longitudinal gages on top of the slab above Girders C, D, and E; four transverse gages on the bottom of the slab perpendicular and adjacent to the tops of Girders C, D, and E; two longitudinal gages on the bottom of the slab adjacent to the sides of Girder D; and longitudinal gages on the outside of the north curb, top of the north parapet, and top of both curbs. Both gage configurations included five deflection gages mounted on the bottom of each girder at Section M. The deflection gages are shown in Fig. 7, and will be referred to as deflectometers.

2.3 STRAIN AND DEFLECTION GAGES

Baldwin-Lima-Hamilton SR-4 resistance-type strain gages, Type A-9-3, were used to gage all of the locations described above, with the exception that the three gages applied to the top of the slab were Type A-9. Each gage location was ground and sanded smooth, followed by thorough cleaning with acetone. SR-4 cement was then used to seal the concrete surface, and to prevent electrical grounding of the gage. After proper drying of the cement, strain gages were dipped in the same SR-4 cement, applied to the prepared surface, and allowed to dry. Gages applied to the rain-exposed surfaces of the roadway and safety curb, were waterproofed with Gage Kote-5. The waterproofing was then cured with a portable heat lamp.

The deflectometers consisted of a strain gage bonded to a flexible, triangular aluminum plate. The aluminum plate was attached to a bar which, in turn, was clamped along the bottom surface of the beam. A detail of the gage mounting is illustrated in Fig. 7. A wire, connected to a 100-lb. weight placed below the gage in the river bed, was attached to the apex of the plate in a deflected position. The deflectometer was calibrated so that the flexural strains of the plates could be converted to girder deflections.

In addition to the active strain and deflection gages described above, there were corresponding temperature compensation gages located near each gage location. Each active gage and temperature compensation gage was connected to one of the 48 channels of monitoring equipment in the BPR equipment trailer. Each channel forms a Wheatstone bridge composed of a power supply, amplifier, oscillator, galvanometer, and the two types of gages described above. As the galvanometer responds to the changes in resistance of the active strain gage, the path of a beam of light is recorded on light-sensitive oscillograph paper. Three variable-speed recording machines are used to record the responses of the 48 gages.

2.4 TEST VEHICLES

The two test vehicles, designated as trucks T1 and T2, are shown in Figs. 8 and 9, respectively. Both vehicles were loaded with steel plates to approximate AASHO Specifications for H20-S16-44 truck loading. Truck T1 was provided by the Bureau of Public Roads, while truck T2 was provided by Schuylkill Products, Inc.

2.5 LOADING LANES

Loading lanes were located on the roadway so that the centerline of the truck would correspond as closely as possible to a girder centerline, or to a line midway between girder centerlines. The centerlines of the seven loading lanes were indicated on the roadway with plastic tape. Figure 2 shows centerlines of the loading lanes to be spaced at 43 inches, with the exception of the outer two lanes, Lanes 1 and 7, which were offset 4 inches toward the bridge centerline to provide better clearance between the curb and the outside face of the tires of a truck being run along these outer lanes. In the AASHO Specifications[1] it is specified that for design purposes, the centerline of a wheel or wheel group may be placed to within 24 inches of the curb face. With vehicle T1 running in Lane 1, this distance was 16.5 inches, while with T2, the clearance was 15.4 inches.

2.6 TIMING AND POSITION INDICATORS

Air hoses were placed 75 feet east and west of gage Section M, in order to monitor the speed of the load vehicle. A timer was actuated as the front axle of an approaching test vehicle passed over the first air hose and was shut off as the truck's front axle passed over the fifth hose. Three additional air hoses, which served as position indicators, were placed at points 50 feet east and west of Section M, as well as at Section M. Each axle passing over one of these hoses caused an abrupt offset from the oscillograph trace representing these indicators. The offsets were then used to correlate the truck position with strain values in the data reduction.

2.7 TEST RUNS

Before and after a set of test runs, the gages were calibrated with no load on the bridge to relate the deflections of the oscillograph traces to base values. During the conduct of static runs, 12 separate calibrations were made.

Crawl runs at a speed of 2 to 3 mph, made with the truck engine idling, were considered to represent the static condition. The oscillograph traces indicated that for the crawl runs, the vibration of the sprung mass of the truck had little effect on strains and deflections. During the crawl runs, the test vehicle was guided by a helper to assure that the truck was centered in the specified loading lane. A view of a crawl run involving the two trucks is shown in Fig. 6. As the front axle of the vehicle neared the first position indicator hose, another helper on the bridge notified the personnel in the trailer to start the recording oscillographs. The recordings were continued until the trailer axle had passed over the third position indicator hose.

Testing was divided into two series, each corresponding to one of the two gage configurations, as described in Section 2.2. Series I testing corresponded to partial gaging at Sections M and N, while Series II testing corresponded to the full gaging at Section M. Table I contains a listing of the runs conducted in both series. Each single-truck run in a particular lane was duplicated by another run in the same series, and by another run, or runs, in the other series. The exception to this procedure was that six two-truck runs were made in Series II with vehicles T1 and T2 passing over the bridge simultaneously.

3. DATA REDUCTION AND EVALUATION

3.1 OSCILLOGRAPH TRACE READING

Data reduction began with the editing of the traces for each test run. Editing required the correlation of trace numbers, each of which represented a particular strain gage, with the traces on the test record. The correlation was facilitated by the existence of trace breaks, corresponding to 16 gage traces and 2 inactive reference traces on each of three oscillograph records from a test run. Some interpretation was necessary where traces overlapped, or trace breaks did not exist. In general, each trace had some definite physical characteristic, such as line weight, which helped to assure the correctness of the interpretation.

With editing completed, all calibration runs were evaluated and compared. The calibration runs consisted of a base record and a calibration record for each gage trace. The distance between a reference trace and the gage trace was measured with an accuracy of 0.01 inch on both records. The calibration value was the difference, always considered positive, between the calibration and base record readings. Since each series of tests extended through a period of several days, calibration values for some gages did not remain constant. Due to this variation of calibration values, only six calibration runs, of the twelve taken during crawl runs, were used. The six calibration runs used were those immediately preceding a set of test runs.

With the completion of editing and the determination of calibration values, the records of test runs could be processed. A no-load reading for each trace was taken at the left side of each record. Most load readings were taken adjacent to the middle drive axle offset, which corresponded to the drive axle passing over the air hose at Section M. Any other vehicle positions were located on the record by proportioning distances from one of the axle offsets, as related to the known axle spacings and the distance between gage sections. Therefore, by distance proportioning, the test vehicle could be positioned at an alternate location in which the rear axle was over Section N.

3.2 EVALUATION OF OSCILLOGRAPH DATA

3.2.1 Strain Distribution and Location of Neutral Axes

For the most efficient method of converting oscillograph traces to strains and deflections, a computer program was written in the WIZ language for use with the GE 225 computer. Gage constants (consisting of gage resistance, gage factor, lead cable length factor, operation attenuation, and calibration attenuation), calibration values, and record readings served as program input data. The program output, consisting of strains and deflections, was listed on prepared cross-sections of the bridge in order to provide a visual check for sizeable errors. The results of several runs were plotted to determine the distribution of the strains along a girder face, as in Figs. 4 and 5.

Another WIZ program was written to calculate the location of the neutral axis at each girder face. The calculation of each value was based on a linear distribution of strain as shown in the strain plots in Figs. 4 and 5. At Section M, with three strain gages, it was possible to use the WIZ program to calculate a neutral axis value from each of three combinations of two strain gages. Each of the three neutral axes was listed as computer printout for comparison. Neutral axis values varying more than 2 inches from the other two corresponding values were eliminated from the averaged value. At Section N only one value of neutral axis was obtained from the two girder face strain gages.

3.2.2 Effective Slab Widths

A third program was developed to calculate the effective slab widths for the girders. Differences in composite girder geometry necessitated separate programs for exterior and interior girders. Both programs accounted for the measured variation of girder depth and slab thickness. In line with experimental results, exterior girders were analyzed as acting compositely with the slab, curb, and parapet, while the interior girders were composite with the slab. The procedure for both programs was similar, as the first section in both programs equated the first moments, with respect to the averaged girder neutral axis, of the tensile and compressive areas of the composite girder, based on the principle of the transformed section. In order to equate these first moments of area, it was necessary to determine the transformed effective width of slab, or

slab, curb, and parapet which was needed to balance the first moment of the tensile area. The transformed effective slab widths of the interior composite girders were calculated by the interior girder program. When the transformed effective slab widths had been calculated for the interior girders, the exterior girder slab widths could be calculated. The transformed effective slab width for an exterior girder depended on the transformed effective slab width of the adjacent interior girder. If the slab width of the adjacent interior girder exceeded 86 inches, the calculated slab width of the exterior girder was less than 84 inches; whereas, if the interior girder slab width was less than or equal to 86 inches, the slab width of the exterior girder was considered to be 84 inches. The dotted lines on the safety curb in Fig. 2 indicate the portions for which effective widths were calculated. The sequence of calculations for the exterior girder was (1) to check whether maximum slab width of 84 inches was required; if so, (2) to check whether the maximum curb width of 33 inches was required; and then if so, (3) to calculate the required width of parapet.

3.2.3 Girder Bending Moments

After the geometry of the composite girder cross-sections had been determined, the next step was to compute the moment carried by each of the girders. For each girder, the location of the neutral axis at each of the two vertical faces, together with the strain distribution on each of the faces, was used to determine both the resultant moment and the inclination of the plane containing the

resultant moment carried by each of the five composite sections. Finally, the component moment acting in the vertical plane was calculated for each girder. The moments computed should be termed moment coefficients, since these coefficients would have to be multiplied by the effective modulus of elasticity, E, of the concrete to determine actual moment values.

Reference to past studies has indicated that efforts to determine a value for the effective E from empirical relationships related to f'_c, or from stress-strain information resulting from cylinder tests, have proved to be fruitless. However, it was possible to determine the effective value by equating the externally applied moment at the cross-section, which can be determined by principles of statics, to the internal resisting moment at the cross-section, which is the product of the sum of the five moment coefficients multiplied by E. After E had been determined, the individual girder moments were calculated for comparison with design values. The average effective modulus used was obtained from all test runs conducted in Series II, with the truck positioned with drive wheels at Section M.

3.2.4 Distribution Coefficients

Distribution coefficients were calculated to determine the percentage of total resisting moment distributed to each girder. The distribution coefficient of a particular girder is the moment coefficient for that girder, divided by the sum of the

moment coefficients for all five girders. It should be noted that the modulus of elasticity was not necessary in this calculation, since dividing the moment for a girder by the sum of five girder moments would result in the same distribution factor.

Evaluation of the distribution coefficients for the Series I testing, where only three of the five girders were gaged, required the superposition of data to obtain moment coefficients for all five girders. Symmetry of the bridge cross-section was assumed. The following example will illustrate this superpositioning procedure. First, see Fig. 2 to recall the relationship of loading lanes to girders. A truck running in Lane 1 produced moment coefficients in Girders C, D, and E, while a truck running in Lane 7 produced moment coefficients in the same girders, which were equivalent, respectively, to the moment coefficients in Girders C, B, and A, with the truck, running in Lane 1. Other symmetric lane loadings in Lanes 2 and 6, and 3 and 5 were combined in the same manner. When moment coefficients had been obtained for all five girders in this manner, a distribution coefficient could be calculated for each girder. Distribution coefficients could only be calculated for loadings in the four Lanes, 1 through 4, to the right of the bridge centerline. The distribution coefficient evaluation for Series II testing was greatly simplified because moment coefficients and distribution coefficients could be calculated directly for all five girders for test runs in all seven lanes. Since the loading lanes and girders were symmetrically located with respect to the centerline of the roadway, it was possible to calculate an average distribution

coefficient by averaging the distribution coefficients of corresponding girders for trucks in symmetrical lanes. For example, it was possible to average the distribution coefficient of Girder E, with a truck in Lane 7, with the distribution coefficient of Girder A, with a truck in Lane 1.

In bridge design specifications, provisions for lateral distribution of load are commonly expressed as distribution factors. These factors are coefficients by which a line of wheel loads is multiplied in computing the design moment for a girder. These distribution factors are based on combinations of loading which will produce the maximum effect in each girder. To enable a comparison of maximum measured moments with the moments obtained from design specifications, the measured distribution coefficients for various lane loadings were either combined to yield maximum distribution factors, or taken directly from the two-truck runs conducted in Series II. The combination of distribution coefficients was done in two ways. In the first, the distribution coefficients resulting from two single lane loadings were combined, so as to correspond to two-truck test runs. In the second, the distribution coefficients resulting from two single truck runs were combined, such that the lateral spacing conformed to AASHO Specification provisions.[1] By the first method, the distribution factors, resulting from the maximum eccentric loading of the bridge, with one of the vehicles in one of the outside Lanes, 1 or 7 with the other in the center Lane 4, could be calculated. Additionally, the distribution factors, resulting from symmetrical loading of the bridge with vehicles in Lanes 2

and 6, could also be calculated. Also, by the second method, the distribution coefficients, resulting from the AASHO Specification provisions for lateral truck spacing, were combined for trucks in Lanes 1 and 5 or Lanes 3 and 7.

4. PRESENTATION OF TEST RESULTS

4.1 DISTRIBUTION COEFFICIENTS

Distribution coefficients are presented both in graph and table form. The graphs show the magnitude of the distribution coefficient plotted for each of the five girders. The load distribution for a particular lane loading is represented by a straight line plot connecting the resultant girder distribution coefficients. The loaded lane is indicated to the right in each plot. To facilitate the interpretation of the distribution coefficient graphs and tables, as well as other tables, a loading key consisting of a diagram showing truck location and direction, and indicating the gage section from which results were obtained, is shown above each graph or table.

Figures 10 through 18 are graphs of Series I single truck test runs for the four right-hand lanes. Distribution coefficients are plotted for both Sections M and N for three types of T1 loading indicated by the loading key: (1) west runs with drive axle at Section M, (2) west runs with rear axle at Section N, and (3) east runs with the drive axle at Section M. Additional Figs. 12, 15, and 18 present a comparison of distribution coefficients at Sections M and N for the test vehicle loaded in Lane 1 and Lane 4. The solid graphs represent distribution coefficients at Section M, while the dotted graphs represent those at Section N.

Figures 19 through 28 represent the distribution coefficients resulting from Series II test runs. Plots are presented for

distribution coefficients resulting directly from a single test vehicle in each of all seven lanes, and from the runs in which the two vehicles were run simultaneously. To check the validity of the distribution coefficients, the averaged distribution coefficients, as explained in Section 3.2.4, are compared with the directly calculated distribution coefficients resulting from test loadings on the right-hand side of the bridge. For example, the averaged value of distribution coefficients for runs in Lanes 1 and 7, and for symmetrical girders for the runs in Lane 4, are compared with coefficients directly resulting from runs in Lanes 1 and 4, respectively. The direct distribution coefficients are plotted as solid lines and the averaged values are plotted as dotted lines.

The distribution coefficients obtained from superimposing runs in both test series are presented in Figs. 29 through 33. A comparison of both directly calculated and averaged distribution coefficients is included for the Series II runs which were superimposed.

The distribution coefficient graphs were plotted from the distribution coefficients listed in Tables 2 through 6. Distribution coefficients at Sections M and N from Series I, and for directly calculated and averaged values from Series II, are listed adjacently for ease of comparison.

4.2 DISTRIBUTION FACTORS

Distribution factors were derived from the distribution coefficients for two trucks proceeding west with drive axles at Section M. The values, either from two-truck runs or from superposition of results from single truck runs, are presented in Table 7. The values represent the placement of test vehicles which produces the maximum moment for each girder. Three groups of listings are shown, corresponding to three types of lateral positioning of the test vehicles. The first group lists the factors for maximum eccentric loading with vehicles in Lanes 1 and 4 or Lanes 4 and 7, as explained in Section 3.2.4. The second group presents factors for trucks in lanes more nearly conforming to AASHO Specification provisions for lateral truck spacing, that is, trucks in Lanes 1 and 5 or Lanes 3 and 7. Factors for all girders for symmetrical loading with vehicles in Lanes 2 and 6 are listed in the third group, which also conforms to AASHO Specification provisions for lateral truck spacing. All three groups include distribution factors obtained from both directly calculated and averaged distribution coefficients.

4.3 SAMPLE GIRDER MOMENTS

In Table 8, the maximum girder moment coefficients and moments for single truck (T1) loading are listed. Table 9 gives values for both the coefficients and moments resulting from loading with two vehicles. The values in the upper part were derived directly from the results of the two-truck runs (T1 and T2), while

values in the lower part resulted from the superposition of values from single truck runs (T1). All girder moments were calculated using a value of 6806.02 ksi for the effective modulus of elasticity of concrete, as obtained by the method explained in Section 3.2.3.

In Table 10, design and experimental live load girder moments taken from Table 9 are compared for the central, outer interior, and exterior girders. The design girder moments were calculated from a free-body diagram of the bridge, using a line of T1 wheel loadings and a distribution factor of 1.30 for the two interior girders and a distribution factor of 0.81 for the exterior girder.

4.4 GIRDER DEFLECTIONS

Experimental girder deflections at Section M are listed in Tables 11 and 12 for trucks in various positions. Values listed for vehicle T1 runs, west and east, are the averages of four runs west and three east, respectively, from both Series I and II testing. The maximum girder deflection for single vehicle loading was 0.077 inches, measured in exterior Girder E with test vehicle T1 running west in Lane 7. Deflections for two-vehicle runs are listed in Table 12. The maximum girder deflection for two-truck loading was 0.129 inches, measured in interior Girder B with test vehicles in Lanes 1 and 4.

4.5 TRANSFORMED EFFECTIVE WIDTHS

Tables 13 through 17 list the average transformed effective width of slab for each girder for each lane loading. The values listed are generally the averaged value of the results from two identical runs. The effective slab width, as defined by the AASHO Specifications for interior girders, is 86 inches.

5. DISCUSSION OF RESULTS

5.1 EXPERIMENTAL STRAINS AND NEUTRAL AXES

The plots of typical strain distribution shown in Figs. 4 and 5 are for vehicle T1 in Lane 7 with the drive axle at Section M, where there are three strain gages along the face of a girder. These plots indicate a linear relationship of strains along the girder faces and into the deck. Figure 4 shows a linear strain distribution between strains at the three gage locations along the girder face of E and the three gages on the parapet and curb above this girder. Figure 5 also shows a linear strain distribution between the gages on both faces of Girder C and the gage on the top of the slab at the centerline of Girder C for the same test load. The linear strain distribution shown in both figures demonstrates that full composite action between the curb, parapet, and slab was effective during the testing program.

The computation of a girder face neutral axis location was based on linear strain distribution. Because there were some small variations between the measured strains resulting from identical vehicle runs, the calculated locations of the neutral axis for a particular face did not always agree. At Section N, where there were only two strain gages on each girder face instead of three, the variation of the neutral axis location was especially noticeable. It is felt that in future tests, at least four strain gages should be applied to the face of each girder in order that variations in

the strains measured at each individual strain gage will have less influence on the determination of the location of the neutral axis.

There were two variations in the location of the girder neutral axis, as determined by points of zero strain on the separate girder faces. The first variation was the inclination of the girder neutral axis between girder faces. The inclination of the girder neutral axis was especially evident in the exterior girders. The second variation was in the location of the average value of the girder face neutral axis locations. Both types of variation depended on the lateral positioning of the test vehicle with respect to a particular girder. The inclination of a girder neutral axis was more nearly horizontal when the girder was directly loaded than when the test vehicle was laterally displaced with respect to that particular girder. The distance from the bottom of a girder to the average location of the neutral axis was usually a maximum, when the girder was directly loaded. This distance generally decreased as the truck was displaced laterally from the particular girder considered.

5.2 DEFLECTIONS

Girder deflections were generally quite small. With a single vehicle on the bridge in one of the exterior loading lanes, the corresponding exterior girder deflected more than any of the other four girders. For two-truck loading of the bridge, with both trucks as close as possible to each other and to the curb (maximum

eccentric loading), the corresponding first interior girder under the loads exhibited maximum deflection. No attempt was made to correlate the lateral distribution of deflections with the distribution coefficients.

5.3 TRANSFORMED EFFECTIVE WIDTH

The magnitude of the transformed effective slab width, as presented in the tables, correlates with the amount of the test load carried by a particular girder. Since the ratio between values of the modulus of elasticity for the cast-in-place deck concrete and the precast, prestressed girder concrete could not be determined for the test structure, it was impossible to determine the actual effective width of the slab. It is possible, for example, if the modulus of the cast-in-place concrete were greater than that of the prestressed girders, that the transformed effective width of the slab might be greater than the actual effective width. If this were the case, the actual effective widths of the slabs of adjacent girders would probably not overlap.

5.4 MODULUS OF ELASTICITY

As explained in Chapter 3, the girder moment coefficients were multiplied by an average effective modulus of elasticity for concrete of 6806.02 ksi, obtained from 41 test runs conducted in Series II. The ACI Code[2] presents a method for the calculation

of modulus of elasticity based on the formula:

$$E_c = w^{1.5}\ 33\ \sqrt{f'_c}\ (\text{psi})$$

If w, the normal weight of concrete, is taken as 145 lb/ft^3 and f'_c is taken as 7021.6 psi, which was the average 28-day strength of the concrete used in the five girders, a value of 4839 ksi is obtained for the elastic modulus of concrete. This value for the modulus is 29% less than the experimentally obtained effective value.

Two of the factors which may be responsible for the difference between the formula value and the experimental effective value are loading rate and stress range. Since an increase in loading rate results in a higher E, it would be expected that the crawl run speeds of the test vehicle would easily exceed the lower rates of loading employed in the development of the formula. Likewise, since the maximum strains produced in the field tests were relatively small, reflecting correspondingly low stresses, the stress range was low. Therefore, the condition would parallel the conditions for which the initial tangent modulus is defined, resulting in a higher value of E.

The field test results are in line with the findings reported in connection with the test of a composite beam (steel) and slab (concrete) bridge in California.[3] In this report, values of E were computed from strain distributions in the slab at both

midspan and quarter-span locations. The average values of the slab concrete were found to be 5980 ksi and 6670 ksi respectively.

The previous explanation might appropriately account for the major part of the discrepancy between experimentally determined internal bending moments and the moments produced by external loads, as described in studies reported by Hulsbos and Linger,[10] and by others.[4,9]

5.5 COMPARISON OF DESIGN AND EXPERIMENTAL LIVE LOAD MOMENTS

The design value of 492.64 kip-ft. for the interior girder live load moment was based on a distribution factor of S/5.5 specified by the PDH, and is equal to the effect at Section M of a line of T1 wheel loads, with the drive axle at Section M, multiplied by 1.30. The distribution factor for an exterior girder, as calculated by PDH Specifications,[11] is 0.81, resulting in a live load design moment of 306.95 kip-ft. for the exterior girders of the test structure.

The experimental live load moment values listed in Table 10 were computed for the two-truck test runs and the combination of single truck runs, corresponding to either the lateral truck spacing of the two-truck test runs or the lateral truck spacing of the AASHO Specification provisions. The maximum moments in Girders A, B, and C were achieved with vehicles T1 and T2 in Lanes 1 and 4. The experimental moments in Girders E, D, and C, with vehicles in Lanes 4 and 7, were smaller than the moments in Girders A, B, and C with

vehicles in Lanes 1 and 4. If the design and experimental girder moments are compared with the experimental values as percentages of the design value, it can be seen that for vehicles in Lanes 1 and 4, the experimental values for interior Girders B and C are significantly less than the design values. For the center Girder C, the average experimental value was 57% of the design value, while for the outer interior Girder B, the average experimental value was 76% of the design value. For exterior Girder A, the maximum experimental value was 172% of the design value.

The second and third combinations of two-truck loading complied more nearly with the AASHO Specification provisions for lateral vehicle spacing. These loading combinations were the superimposed T1 vehicle runs in either Lanes 1 and 5 or Lanes 2 and 6, the latter loading combination corresponding to runs conducted with two trucks simultaneously on the bridge. For these two loading combinations the maximum experimental moment values in Girders A and B were achieved by the superimposing of T1 vehicle runs in Lanes 1 and 5, while the maximum experimental moment in Girder C was achieved with vehicle T1 in Lanes 2 and 6. For both interior girders the experimental moment values were nearly the same for both combinations of loading, the experimental moment averaging 53% of the design moment for Girder C and 68% of the design moment for Girder B. For exterior Girder A, the maximum experimental moment was 142% of the design value.

The maximum experimental girder moments were developed

in the exterior girder when trucks were run in either Lanes 1 and 4 or Lanes 1 and 5.

These comparisons of experimental and design girder moments would be valid, in general, for vehicles of the type utilized and for medium span bridges. The vehicles used for testing were approximations of AASHO specified H20-S16-44 axle spacings and loadings. A test vehicle with a shorter wheelbase between the trailer and drive axles, such as the 14-ft. wheelbase specified by AASHO, and with axles loaded to H20-S16-44 loads would produce slightly greater girder moments. However, it is felt that the distribution coefficients would be affected very little.

5.6 DISTRIBUTION COEFFICIENTS

The distribution of load, for Series I runs, was somewhat affected by the localized influence of the truck axles. The effect of this localized influence was especially noted for single trucks running along the center Lane 4. For either an eastbound or westbound vehicle with the drive axles at Section M, the load distribution at Section N was more uniform than at Section M. With the trailer axle located at Section N, load distribution was more uniform at Section M than at Section N. When single vehicles with the drive axle at Section M were considered in the lanes offset from Lane 4, the distribution coefficient for the exterior girder was generally larger at Section N than at Section M. However, for maximum moment loading, the applied girder moment at Section N would be less than

that at Section M. In general, there was no significant variation between the distribution coefficients calculated near midspan and near the quarter-point of the span.

A comparison of distribution coefficients resulting from single truck runs during Series II enabled a check on the actual symmetry of the bridge. The slight lack of symmetry can be seen in the distribution coefficient graphs. Generally, girders on the right side of the section carried more load than those on the left side. For instance, the sum of distribution coefficients for Girders A, B, and C with a vehicle in Lane 1 was about 2 to 3 percent greater than the corresponding sum for Girders E, D, and C with a vehicle in Lane 7. Although there is a slight variation of load distribution for vehicles in symmetrical loading lanes, the averaged distribution coefficients do not differ significantly from the directly obtained values.

The distribution coefficients resulting from the Series II two-truck runs were greatest for the exterior girder when the bridge was loaded in Lanes 1 and 4. The averaged distribution coefficients for the two-truck runs were not significantly different from the directly obtained values. The distribution coefficients resulting from the superimposed runs of single vehicles were not significantly different from the corresponding coefficients resulting from the two-truck runs. The correlation of distribution coefficients for two-truck runs with vehicles T1 and T2 and for the superimposed single vehicle runs with the same vehicles was especially good.

Reasonable correlation was also obtained for the distribution coefficients resulting from the superimposing of runs with vehicles T1 and T2 and the coefficients resulting from the superimposing of T1 vehicle runs.

5.7 DISTRIBUTION FACTORS

The design distribution factors for a truck-wheel loading were established as 1.30 for the interior girders and 0.81 for the exterior girders for the Drehersville test structure. The experimental distribution factors listed in Table 7 were calculated from runs made with two trucks or two superimposed trucks proceeding westward with the drive axles at Section M. Both the directly calculated and average distribution factors resulting from this maximum loading are presented to implement a comparison of values.

The two-truck test loading and the superimposed single vehicle loadings, with vehicles in either Lanes 1 and 4 or Lanes 4 and 7, result in the maximum experimentally determined distribution factors for any of the test structure girders. For these critical loading cases, the distribution factors for exterior Girders A and E exceed the design value of 0.81, while the interior girder design distribution factor of 1.30 exceeds the resultant experimental distribution factors for interior Girders B, C, and D. The maximum experimental values for this loading case were 1.37 for exterior Girder A and 0.98 and 0.77 for interior Girders B and C, respectively. The maximum experimental distribution factors resulting from two-truck runs conforming to AASHO Specification provisions

for lateral vehicle spacing were 1.22 for exterior Girder A and 0.88 and 0.70 for interior Girders B and C, respectively.

6. SUMMARY AND CONCLUSIONS

6.1 SUMMARY

The primary objective of this pilot study was to determine the lateral distribution of the live load to the precast, prestressed concrete spread box girders in a typical bridge constructed according to the bridge design standards of the Pennsylvania Department of Highways. A secondary objective was the evaluation of testing and data reduction procedures in establishing the behavior of the bridge subjected to design-load vehicles.

This report presents the results of a field test program conducted on an existing bridge located near Drehersville, Pennsylvania. The bridge was basically composed of a reinforced concrete slab supported by five prestressed concrete girders, and had reinforced concrete curb and parapet sections. Two test vehicles, simulating AASHO H20-S16-44 loading, were driven across the span singly and in combination at crawl speeds of 2-3 mph along seven approximately equally spaced lanes. The testing was divided into two series corresponding to two different strain gage configurations. In Series I three of the five girders were fully gaged at two different cross-sections, while in Series II all five girders were fully gaged at one cross-section. In addition, other gages were mounted at various locations on the deck, curb, and parapet during both series. The strain variations resulting from the various truck runs were measured with continuous strain recording equipment supplied by the

U. S. Bureau of Public Roads. The distribution of the strains was evaluated to determine the locations of the girder neutral axes, from which the effective transformed areas of slab, curb and parapet portions of the bridge deck could be calculated. Girder moment coefficients were then calculated and combined for comparison with design values. Experimental girder distribution coefficients were then computed and maximum experimental girder distribution factors were developed and compared with design distribution factors calculated according to PDH design specifications.

6.2 CONCLUSIONS

The following conclusions were made from the results of the pilot study crawl runs:

1. The test results revealed that the actual distribution factors for the girders were significantly different from the values used in the design of the structure. The magnitude of the difference is sufficient to conclude that the testing of other structures of the same type will yield similar information. The reader is cautioned that this report covers the results of crawl run testing only. However, a preliminary evaluation of data from speed runs conducted as another part of the same field test program indicated that the distribution factors will not be affected significantly by faster moving vehicles.

2. The test results consistently indicated full composite action between the slab and the curb sections, and between curb and

parapet sections. This action is undoubtedly one of the primary reasons for the difference between experimental and design values of the distribution factors. Ignoring the composite action in design does not necessarily result in a conservative design. That is, it is possible that higher stresses than those computed in the design would be produced in the exterior girder, even though stresses lower than design values would be produced in the interior girders.

3. A review of the tables listing effective slab widths indicates (1) that for this structure, the center-to-center spacing of the girders is a reasonably accurate estimate of the effective slab width, and (2) that use of the same value of E for both beam and slab concrete is also reasonable.

4. For testing at crawl speed, the superimposing of the results of single truck runs to determine the effects of two-truck loading is a valid procedure.

5. The strain measurements taken at a cross-section having half of the girders gaged can be combined to accurately represent measurements taken with all girders gaged.

6. At least four strain gages should be applied to the face of a girder in order to accurately establish the location of the neutral axis.

7. ACKNOWLEDGMENTS

This study was conducted in the Department of Civil Engineering at Fritz Engineering Laboratory, under the auspices of the Lehigh University Institute of Research, as part of a research investigation sponsored by: the Pennsylvania Department of Highways, the U. S. Department of Commerce, Bureau of Public Roads, and the Reinforced Concrete Research Council.

The experimental work was conducted under the direction of Dr. C. L. Hulsbos, formerly Research Professor of Civil Engineering, Lehigh University, in cooperation with Messrs. R. F. Varney and C. F. Galambos, Structural Research Engineers, Bureau of Public Roads.

The field test equipment, including the recording equipment and the main test vehicles, were made available through the cooperation of Mr. C. F. Scheffey, Chief, Structures and Applied Mechanics Division, Office of Research and Development, Bureau of Public Roads. The equipment was operated by Messrs. R. F. Varney, C. F. Galambos, and Harry Laatz. The second test vehicle was made available by Mr. Joseph Nagle, President, Schuylkill Products, Inc.

The basic planning in this investigation was in cooperation with Mr. K. H. Jensen, Bridge Engineer, and Mr. H. P. Koretzky, Engineer in charge of Prestressed Concrete Structures, both of the Bridge Engineering Department, Pennsylvania Department of Highways.

The following Lehigh University personnel were associated with this study. Mr. A. A. Guilford was the Principal Investigator on the project; Dr. J. M. Hanson, Dr. J. C. Badoux, and Mr. Howard Brecht, assisted in the field testing; Messrs. T. W. Schaffer, S. H. Cowen, and R. J. Dietz assisted in the data reduction and computer programming; and Mrs. Carol Kostenbader typed the manuscript.

8. TABLES

Table 1 Listing of Test Runs

Vehicle	Direction	Lanes	Number
	Series I		
T1	West	1 through 7	14*
T1	East	1 through 7	14*
			28
	Series II		
T1	West	1 through 7	14*
T1	East	1 through 7	7
T2	West	1 through 7	14*
	Two Truck Runs		
T1 and T2	West	4 (T1) 1 (T2)	2
T1 and T2	West	6 (T1) 2 (T2)	2
T1 and T2	West	4 (T1) 7 (T2)	2
			41

* Two runs per lane

Table 2 Distribution Coefficients for Single-Truck Runs, Series I

$$\text{Distribution Coefficient} = \frac{\text{Moment Coefficient}}{\Sigma \text{ Moment Coefficients}} (100)$$

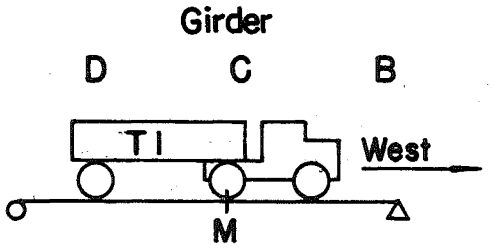

	E	D	C	B	A
Lane 1	7.67	9.80	14.90	27.28	40.35
Lane 2	10.37	11.74	18.36	28.99	30.56
Lane 3	13.62	15.68	23.09	24.72	22.89
Lane 4	17.88	19.09	26.06	19.09	17.88

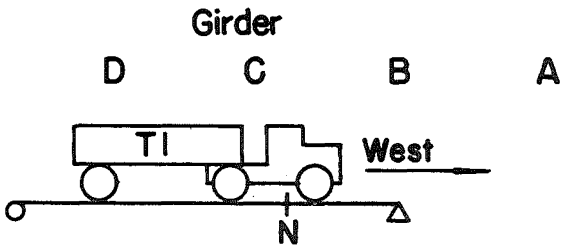

	E	D	C	B	A
Lane 1	9.46	8.76	15.26	25.40	41.12
Lane 2	12.16	11.47	18.14	24.18	34.05
Lane 3	17.13	15.80	20.00	20.85	26.22
Lane 4	20.28	19.22	21.00	19.22	20.28

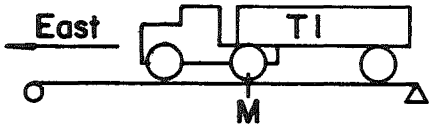

	E	D	C	B	A
Lane 1	8.92	9.44	14.89	30.36	36.39
Lane 2	9.18	11.39	18.82	30.76	29.85
Lane 3	12.22	16.22	23.86	26.60	21.10
Lane 4	15.59	20.87	27.08	20.87	15.59

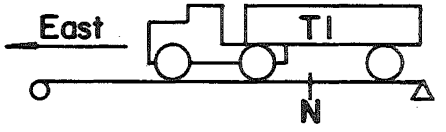

	E	D	C	B	A
Lane 1	9.08	9.61	16.23	26.27	38.81
Lane 2	10.40	11.18	18.88	26.44	33.10
Lane 3	13.96	15.29	21.82	24.52	24.41
Lane 4	19.19	19.28	23.06	19.28	19.19

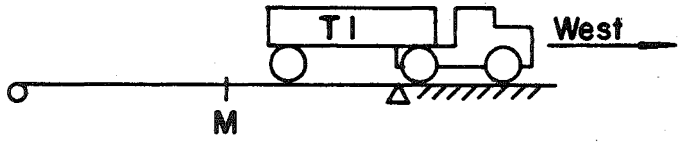

	E	D	C	B	A
Lane 1	7.26	11.15	16.73	27.44	37.42
Lane 2	10.69	11.96	18.44	26.58	32.33
Lane 3	13.32	15.74	18.21	20.34	32.39
Lane 4	18.94	20.34	21.44	20.34	18.94

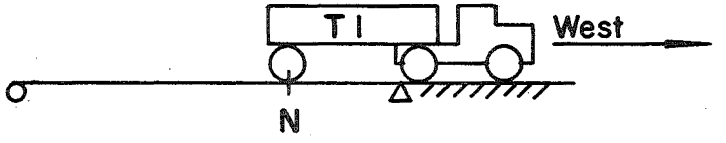

	E	D	C	B	A
Lane 1	8.20	5.42	11.42	29.45	45.51
Lane 2	10.28	7.16	15.39	35.72	31.45
Lane 3	14.07	12.20	26.80	28.49	18.44
Lane 4	18.03	16.84	30.26	16.84	18.03

Table 3 Distribution Coefficients for Single-Truck Runs, Series II

$$\text{Distribution Coefficient} = \frac{\text{Moment Coefficient}}{\Sigma \text{ Moment Coefficients}} (100)$$

	Directly Calculated Values					Averaged Values				
	Girder					Girder				
	E	D	C	B	A	E	D	C	B	A
					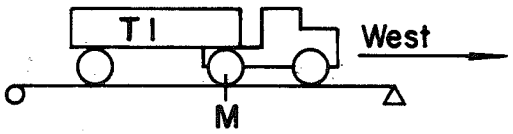					
Lane 1	7.63	8.78	12.40	27.96	43.22	7.78	9.23	12.75	27.06	43.18
Lane 2	11.51	11.14	16.37	30.20	30.78	11.12	11.91	16.87	28.48	31.62
Lane 3	13.35	14.25	21.12	26.91	24.37	13.56	15.21	21.59	25.74	23.90
Lane 4	17.64	18.10	23.82	21.17	19.27	18.45	19.64	23.82	19.64	18.45
Lane 5	23.42	24.58	22.06	16.16	13.78					
Lane 6	32.47	26.76	17.37	12.69	10.71					
Lane 7	43.13	26.15	13.10	9.68	7.94					
					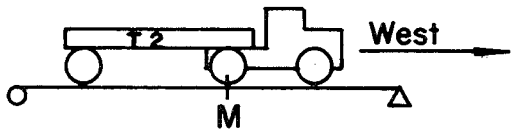					
Lane 1	7.13	8.21	12.54	24.65	47.47	8.00	8.91	13.19	25.58	44.32
Lane 2	10.64	10.92	17.10	26.04	35.30	11.24	11.28	17.22	26.35	33.91
Lane 3	13.11	13.54	21.80	25.70	25.85	13.66	14.24	22.45	24.73	24.92
Lane 4	17.28	17.60	25.24	20.46	19.42	18.35	19.03	25.24	19.03	18.35
Lane 5	24.00	23.76	23.10	14.93	14.21					
Lane 6	32.52	26.66	17.34	11.65	11.83					
Lane 7	41.17	26.51	13.84	9.60	8.88					

Table 4 Distribution Coefficients for Single-Truck Runs, Series II (continued)

$$\text{Distribution Coefficient} = \frac{\text{Moment Coefficient}}{\Sigma \text{ Moment Coefficients}} (100)$$

	Directly Calculated Values					Averaged Values				
	Girder					Girder				
	E	D	C	B	A	E	D	C	B	A
				East T1 M						
Lane 1	6.21	8.81	12.45	28.32	44.21	6.70	8.92	12.58	27.46	44.34
Lane 2	8.40	10.21	16.11	30.26	35.02	9.69	11.31	16.26	28.59	34.15
Lane 3	11.44	14.25	22.09	28.72	23.50	12.49	15.27	22.42	27.18	22.64
Lane 4	17.11	18.82	24.48	21.48	18.11	17.61	20.15	24.48	20.15	17.61
Lane 5	21.77	25.64	22.74	16.30	13.55					
Lane 6	33.28	26.92	16.42	12.40	10.98					
Lane 7	44.47	26.59	12.71	9.04	7.19					
				T1 West M						
Lane 1	8.43	9.18	14.30	26.18	41.91	9.72	10.20	15.57	25.40	39.11
Lane 2	12.16	11.79	17.06	25.33	33.66	13.40	12.91	18.47	24.65	30.57
Lane 3	16.20	15.15	17.98	22.74	27.93	17.15	15.99	18.82	21.67	26.37
Lane 4	21.32	17.72	18.98	20.22	21.76	21.54	18.97	18.98	18.97	21.54
Lane 5	24.81	20.60	19.65	16.83	18.11					
Lane 6	27.48	23.97	19.87	14.04	14.64					
Lane 7	36.31	24.62	16.83	11.22	11.02					

Table 5 Distribution Coefficients for Two-Truck Runs, Series II

$$\text{Distribution Coefficient} = \frac{\text{Moment Coefficient}}{\Sigma\,\text{Moment Coefficients}}\,(100)$$

	Directly Calculated Values — Girder					Averaged Values — Girder				
	E	D	C	B	A	E	D	C	B	A
					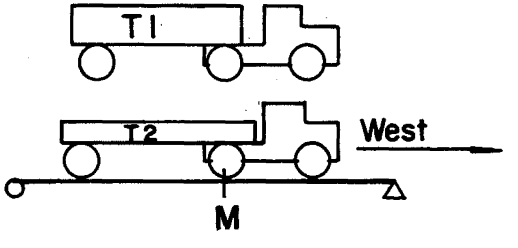					
Lane 1 and 4	12.57	12.60	18.32	22.37	34.14	13.72	13.58	18.74	22.10	31.86
Lane 2 and 6	21.25	18.06	17.36	20.32	23.01	22.13	19.19	17.36	19.19	22.13
Lane 4 and 7	29.57	21.82	19.16	14.57	14.88					
					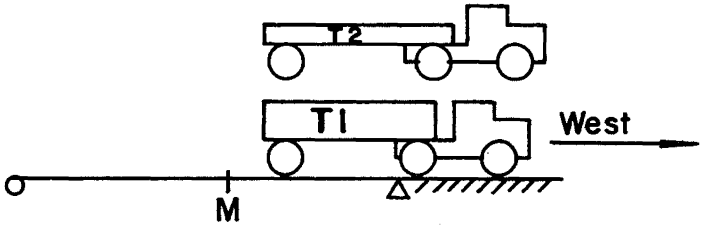					
Lane 1 and 4	16.10	13.24	16.27	21.62	32.77	16.91	13.92	16.70	21.31	31.16
Lane 2 and 6	21.98	16.54	17.00	19.77	24.71	23.34	18.16	17.00	18.16	23.34
Lane 4 and 7	29.56	21.00	17.12	14.61	17.71					

Table 6 Distribution Coefficients for Superimposed Single-Truck Runs

$$\text{Distribution Coefficient} = \frac{\text{Moment Coefficient}}{\sum \text{Moment Coefficients}} (100)$$

	Directly Calculated Values, Girder E	D	C	B	A	Averaged Values, Girder E	D	C	B	A
					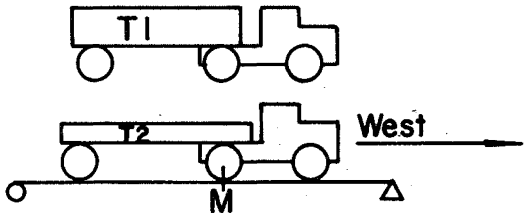					
Lane 1 and 4	12.38	13.16	18.18	22.92	33.36	13.23	14.28	18.50	22.61	31.38
Lane 1 and 5	15.27	16.40	17.30	20.41	30.62	15.95	17.32	17.39	20.40	28.94
Lane 2 and 6	21.55	18.84	17.24	19.36	23.01	21.43	19.88	17.05	19.13	22.51
Lane 3 and 7	27.26	20.38	17.48	18.26	16.62					
Lane 4 and 7	29.41	22.30	18.83	15.39	14.07					
					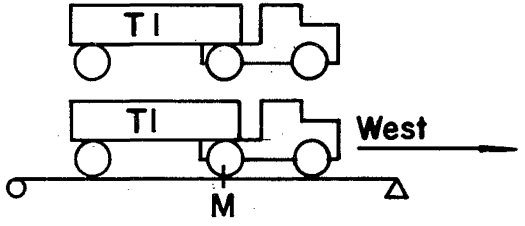					
Lane 1 and 4	12.78	14.45	20.48	23.18	29.11					
Lane 1 and 5	15.28	17.26	19.00	21.48	26.98	Series I				
Lane 2 and 6	20.46	20.36	18.36	20.36	20.46					
Lane 1 and 4	12.64	13.44	18.11	24.57	31.24	13.11	14.44	18.28	23.35	30.82
Lane 1 and 5	15.53	16.68	17.23	22.06	28.50	15.84	17.48	17.17	21.14	28.37
Lane 2 and 6	21.99	18.95	16.87	21.44	20.75	21.37	20.19	16.88	20.19	21.37
Lane 3 and 7	28.24	20.20	17.11	18.30	16.15					
Lane 4 and 7	30.39	22.13	18.46	15.42	13.60	Series II				

Table 7 Experimental Distribution Factors

Section M - Truck Moving West

LOAD	LANE	DIRECTLY CALCULATED VALUES GIRDER A	B	C	D	E	AVERAGE VALUES GIRDER A	B	C	D	E
BASED ON MINIMUM LATERAL TRUCK SPACING											
Test T1,T2	(1,4)	1.37	0.89	0.73			1.27	0.88	0.75		
	(4,7)			0.77	0.87	1.18					
Super T1,T2	(1,4)	1.33	0.92	0.73			1.26	0.90	0.74		
	(4,7)			0.75	0.89	1.18					
Super T1,T1	(1,4)	1.25	0.98	0.72			1.23	0.93	0.73		
	(4,7)			0.74	0.88	1.22					
BASED ON AASHO PROVISIONS FOR LATERAL TRUCK SPACING											
Super T1,T2	(1,5)	1.22	0.82	0.69	0.66		1.16	0.82	0.70	0.69	
	(3,7)		0.73	0.70	0.82	1.09					
Super T1,T1	(1,5)	1.14	0.88	0.69	0.67		1.13	0.85	0.69	0.70	
	(3,7)		0.73	0.68	0.81	1.13					
Test T1,T2	(2,6)	0.92	0.81	0.69	0.72	0.85	0.89	0.77	0.69	0.77	0.89
Super T1,T2	(2,6)	0.92	0.77	0.69	0.75	0.86	0.90	0.77	0.68	0.80	0.86
Super T1,T1	(2,6)	0.83	0.86	0.67	0.76	0.88	0.85	0.81	0.68	0.81	0.85

Table 8 Sample Girder Moment Coefficients and Moments, Single-Truck Runs

Effective Modulus of Elasticity = 6,806.02 ksi

	Moment Coefficient (10^{-6} ft.-in^2)					Moment (kip-ft.)				
	Girder					Girder				
	E	D	C	B	A	E	D	C	B	A
Lane 1	8656	9946	14018	31524	48943	58.916	67.691	95.407	214.553	333.108
Lane 2	13173	12740	18719	34516	35189	89.658	86.706	127.400	234.915	239.500
Lane 3	15260	16278	24115	30734	27849	103.857	110.790	164.130	209.178	189.539
Lane 4	19389	19906	26204	23285	21160	131.963	135.480	178.348	158.479	144.012
Lane 5	25344	26436	23724	17497	14923	172.489	179.923	161.470	119.086	101.566
Lane 6	36646	30216	19608	14325	12110	249.414	205.652	133.455	97.499	82.423
Lane 7	46492	28177	14113	10435	8544	316.428	191.773	96.053	71.018	58.152

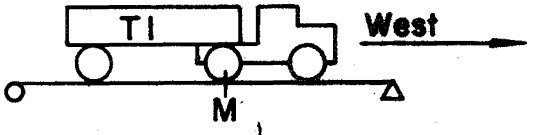

Table 9 Sample Girder Moment Coefficients and Moments, Two-Truck Runs and Superimposed Single-Truck Runs

Effective Modulus of Elasticity = 6,806.02 ksi

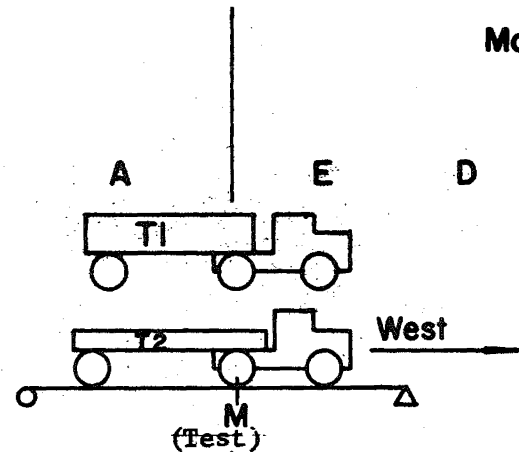

	Moment Coefficient (10^{-6} ft.-in.^{2})					Moment (kip-ft.)				
	Girder					Girder				
	E	D	C	B	A	E	D	C	B	A
Lane 1 and 4	28510	28580	41563	50764	77472	194.040	194.514	282.882	345.498	527.278
Lane 2 and 6	45736	38880	37381	43717	49502	311.282	264.616	254.414	297.541	336.912
Lane 4 and 7	64030	47221	41468	31537	32205	435.788	321.389	282.232	214.641	219.190

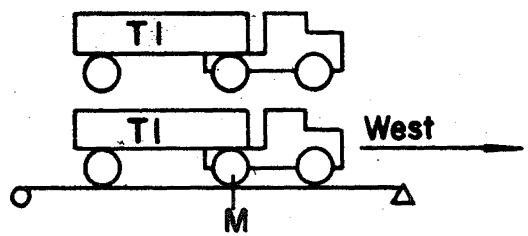

(Superposition)

Lane 1 and 5	231.405	247.614	256.877	333.639	434.674
Lane 2 and 6	339.082	291.358	260.855	332.414	321.923
Lane 3 and 7	420.285	302.563	260.183	280.196	247.691

Table 10 Comparison of Design and Experimental Girder Moments

Section M

	DESIGN MOMENT kip-ft.	EXPERIMENTAL MOMENT kip-ft	EXPERIMENTAL / DESIGN
INTERIOR GIRDER C			
Test T1,T2			
Lanes 1 and 4	492.64	282.88	0.574
Superposition T1,T1			
Lanes 1 and 4	492.64	273.76	0.556
Superposition T1,T1			
Lanes 1 and 5	492.64	256.88	0.521
Lanes 2 and 6	492.64	260.86	0.530
INTERIOR GIRDER B			
Test T1,T2			
Lanes 1 and 4	492.64	345.50	0.701
Superposition T1,T1			
Lanes 1 and 4	492.64	373.03	0.757
Superposition T1,T1			
Lanes 1 and 5	492.64	333.64	0.677
Lanes 2 and 6	492.64	332.41	0.675
EXTERIOR GIRDER A			
Test T1,T2			
Lanes 1 and 4	306.95	527.28	1.718
Superposition T1,T1			
Lanes 1 and 4	306.95	477.12	1.554
Superposition T1,T1			
Lanes 1 and 5	306.95	434.67	1.416
Lanes 2 and 6	306.95	321.92	1.049

Table 11 Girder Deflections, Single-Truck Runs

(All values in inches)

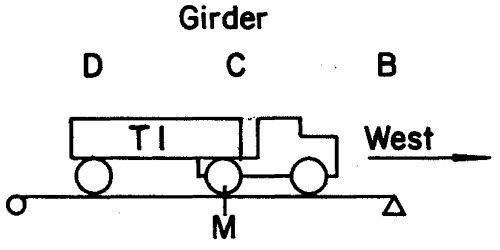

	E	D	C	B	A
Lane 1	0.02034	0.03058	0.05000	0.06990	0.07535
Lane 2	0.02466	0.03676	0.05801	0.07158	0.06347
Lane 3	0.03161	0.04585	0.06572	0.06598	0.05050
Lane 4	0.04044	0.05517	0.07002	0.05736	0.03977
Lane 5	0.05218	0.06392	0.06562	0.04638	0.03070
Lane 6	0.06491	0.06808	0.05787	0.03696	0.02414
Lane 7	0.07724	0.06764	0.04984	0.02926	0.01873

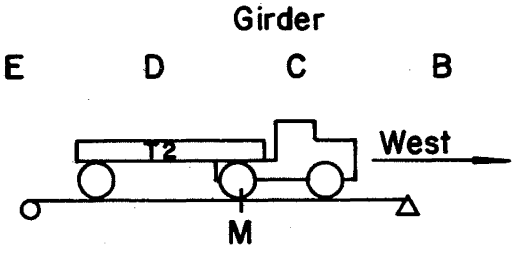

	E	D	C	B	A
Lane 1	0.01835	0.02844	0.04595	0.06698	0.07228
Lane 2	0.02349	0.03499	0.05527	0.06963	0.06036
Lane 3	0.02986	0.04363	0.06364	0.06450	0.04845
Lane 4	0.02814	0.05376	0.06727	0.05719	0.03794
Lane 5	0.04993	0.06240	0.06316	0.04600	0.02979
Lane 6	0.06192	0.06701	0.05606	0.03714	0.02321
Lane 7	0.07366	0.06582	0.04769	0.02999	0.01913

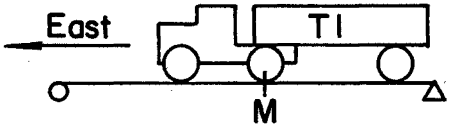

	E	D	C	B	A
Lane 1	0.01793	0.02675	0.04284	0.06430	0.06726
Lane 2	0.02163	0.03218	0.04984	0.06444	0.05586
Lane 3	0.02590	0.03896	0.05622	0.05860	0.04328
Lane 4	0.03444	0.04802	0.06028	0.05074	0.03384
Lane 5	0.04576	0.05615	0.05678	0.04074	0.02648
Lane 6	0.05714	0.06043	0.05003	0.03339	0.02156
Lane 7	0.06748	0.05889	0.04303	0.02740	0.01616

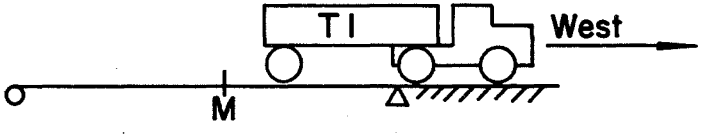

	E	D	C	B	A
Lane 1	0.00946	0.01466	0.02440	0.03532	0.03806
Lane 2	0.01140	0.01730	0.02810	0.03578	0.03155
Lane 3	0.01516	0.02282	0.03307	0.03341	0.02477
Lane 4	0.01952	0.02680	0.03566	0.02866	0.01958
Lane 5	0.02522	0.03145	0.03306	0.02322	0.01510
Lane 6	0.03201	0.03247	0.02818	0.01793	0.01186
Lane 7	0.03952	0.03299	0.02432	0.01478	0.00959

Table 12 Girder Deflections, Two-Truck Runs

(All values in inches)

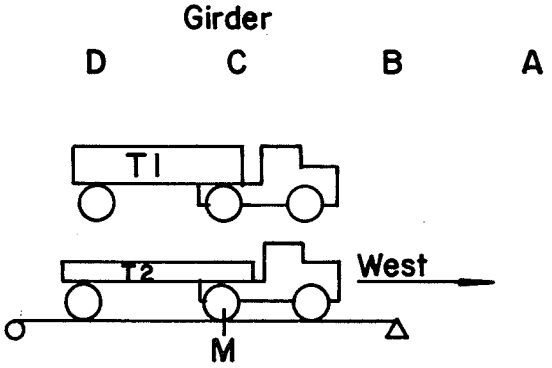

Lane 1 and 4	0.05898	0.08443	0.11718	0.12900	0.11383
Lane 2 and 6	0.08884	0.10677	0.11465	0.10197	0.08655
Lane 4 and 7	0.11405	0.12419	0.11828	0.09139	0.05927

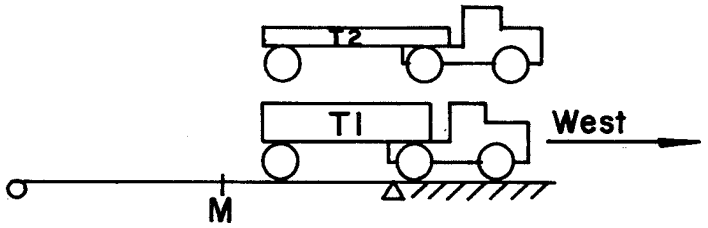

Lane 1 and 4	0.02986	0.04200	0.06048	0.06776	0.06084
Lane 2 and 6	0.04405	0.05302	0.05986	0.05906	0.04626
Lane 4 and 7	0.06021	0.06404	0.06112	0.04647	0.02979

Table 13 Transformed Effective Slab Widths, Series I

(All values in inches)

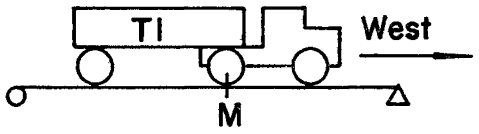

	Girder E	Girder D	Girder C
Lane 1	84.00	64.46	67.01
Lane 2	84.00	63.74	70.81
Lane 3	84.00	73.38	75.50
Lane 4	84.00	81.15	78.29
Lane 5	78.93	96.13 *	94.22
Lane 6	71.66	110.68 *	68.30
Lane 7	76.20	101.60	47.0

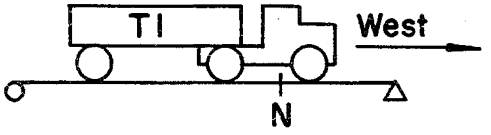

	Girder E	Girder D	Girder C
Lane 1	84.00	44.64	55.42
Lane 2	84.00	58.18	58.36
Lane 3	84.00	69.98	61.96
Lane 4	84.00	62.52	62.24
Lane 5	84.00	63.82	59.84
Lane 6	84.00	81.60	65.46
Lane 7	84.00	77.04	50.90

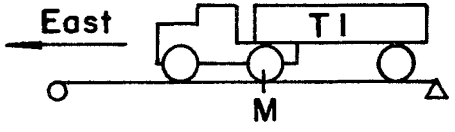

	Girder E	Girder D	Girder C
Lane 1	84.00	51.97	56.80
Lane 2	64.18	56.20	65.04
Lane 3	83.12	80.24	88.05
Lane 4	81.44	91.12 *	84.19
Lane 5	76.86	100.26 *	89.28
Lane 6	76.51	100.98	68.26
Lane 7	67.28	119.45 *	57.16

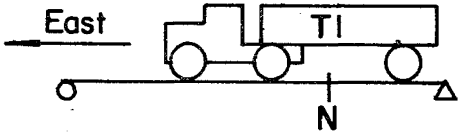

	Girder E	Girder D	Girder C
Lane 1	84.00	45.76	55.68
Lane 2	81.06	45.64	52.84
Lane 3	84.00	53.80	61.96
Lane 4	84.00	60.02	64.28
Lane 5	84.00	67.06	69.24
Lane 6	84.00	79.14	56.02
Lane 7	81.76	85.78	65.10

* Overlap of transformed effective width.

Table 14 Transformed Effective Slab Widths (continued), Series I

(All values in inches)

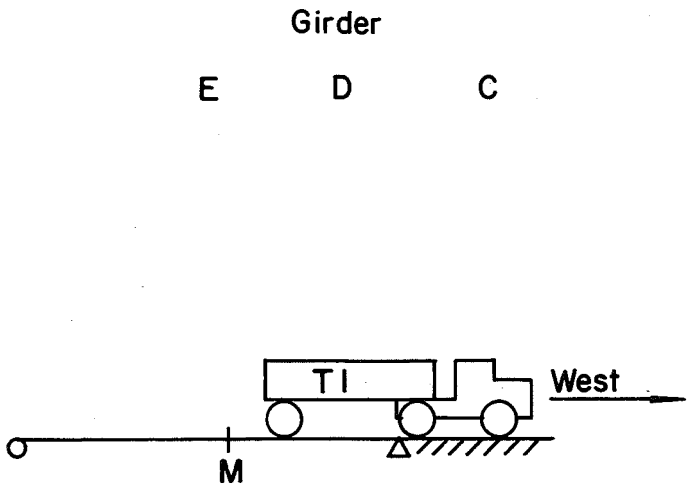

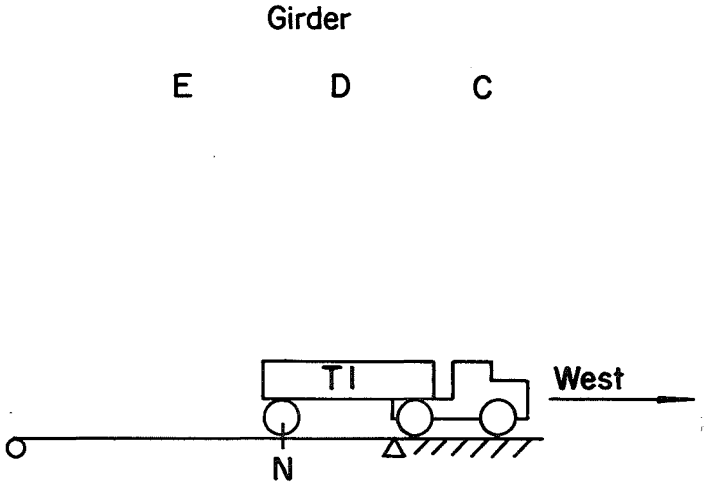

Lane 1	65.87	59.25		57.45	84.00	51.13	43.74
Lane 2	70.56	61.00		56.11	72.12	49.48	48.90
Lane 3	84.00	70.65		56.36	82.18	76.62	84.70
Lane 4	84.00	75.79		89.20	84.00	64.84	75.64
Lane 5	78.92	96.15		69.31	82.38	89.23	78.11
Lane 6	72.24	109.52	*	75.42	77.34	99.32	62.34
Lane 7	84.00	81.20		43.61	84.00	80.15	53.89

* Overlap of transformed effective width

Table 15 Transformed Effective Slab Widths, Series II

(All values in inches)

Girder

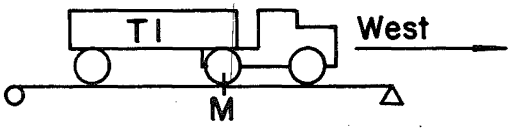

Lane 1	74.64	50.13	46.44	96.20	78.90
Lane 2	84.00	60.30	56.93	94.41	79.80
Lane 3	84.00	75.48	92.54 *	105.76	74.12
Lane 4	82.52	84.08	74.90	73.44	84.00
Lane 5	72.55	108.90 *	89.28	61.94	84.00
Lane 6	73.70	106.62 *	73.82	64.02	84.00
Lane 7	75.58	102.84	58.70	49.65	84.00

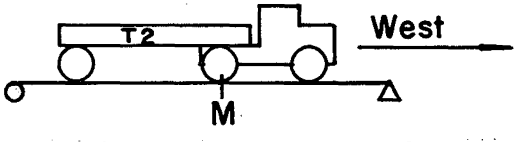

Lane 1	84.00	56.20	59.86	98.98	77.42
Lane 2	84.00	60.58	67.69	98.52	77.74
Lane 3	84.00	71.29	91.29 *	101.31	76.34
Lane 4	84.00	72.70	83.40	76.37	84.00
Lane 5	72.95	108.10 *	90.26	58.08	84.00
Lane 6	73.20	107.62 *	73.84	52.86	84.00
Lane 7	74.42	105.18	60.24	46.26	84.00

* Overlap of transformed effective width

Table 16 Transformed Effective Slab Widths (continued), Series II

(All values in inches)

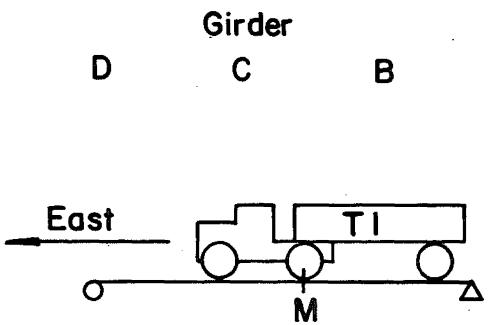

Lane 1	84.00	65.44	52.91	104.74	74.63
Lane 2	84.00	55.49	61.05	83.08	84.00
Lane 3	84.00	66.64	94.64 *	102.76 *	75.62
Lane 4	84.00	78.31	72.78	79.08	84.00
Lane 5	73.47	107.08 *	93.79 *	72.26	84.00
Lane 6	75.36	103.28 *	74.12 *	59.27	84.00
Lane 7	60.26	133.49 *	62.79 *	44.07	84.00

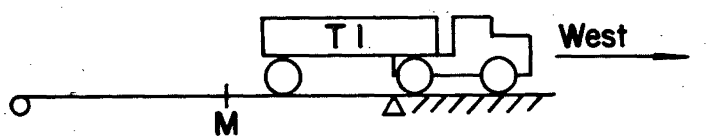

Lane 1	74.75	104.50 *	68.89 *	95.94	76.38
Lane 2	84.00	63.19	60.96	103.32	75.34
Lane 3	77.52	91.86 *	86.44 *	108.36 *	72.82
Lane 4	78.29	84.68	81.20	71.86	83.73
Lane 5	76.18	84.44	67.96	52.01	84.00
Lane 6	72.04	109.93 *	94.90 *	81.95 *	77.70
Lane 7	84.00	78.46	57.86	47.40	84.00

* Overlap of transformed effective width

Table 17 Transformed Effective Slab Widths (continued), Series II

(All values in inches)

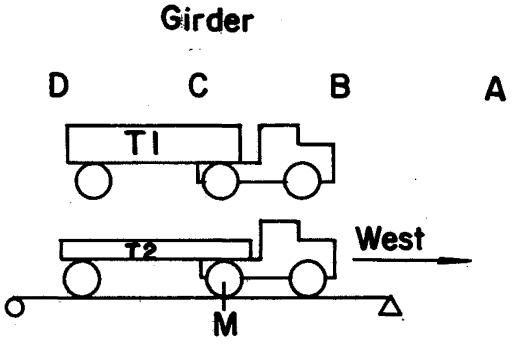

Lane 1 and 4	84.00	73.56	77.60	87.25	83.38
Land 2 and 6	83.32	87.15	66.39	77.15	84.00
Lane 4 and 7	78.06	97.86	70.17	60.57	84.00

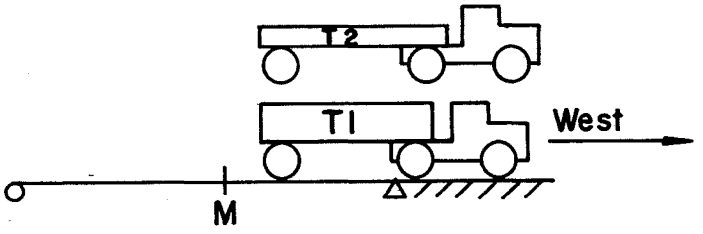

Lane 1 and 4	84.00	70.75	66.69	73.58	84.00
Lane 2 and 6	84.00	72.88	62.25	70.56	84.00
Lane 4 and 7	84.00	82.32	67.38	55.44	84.00

9. FIGURES

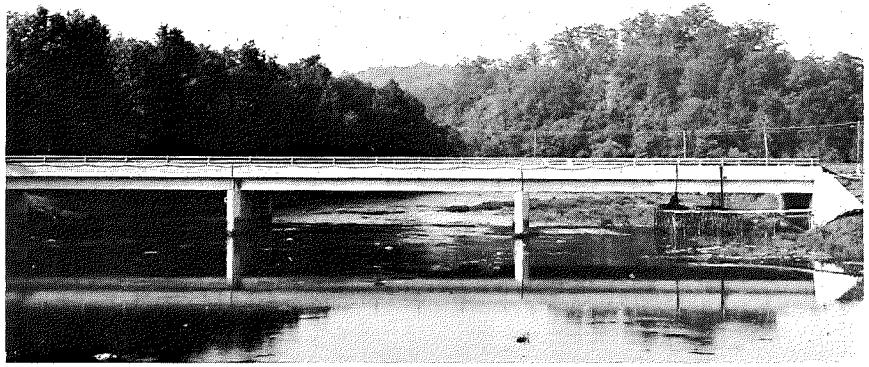

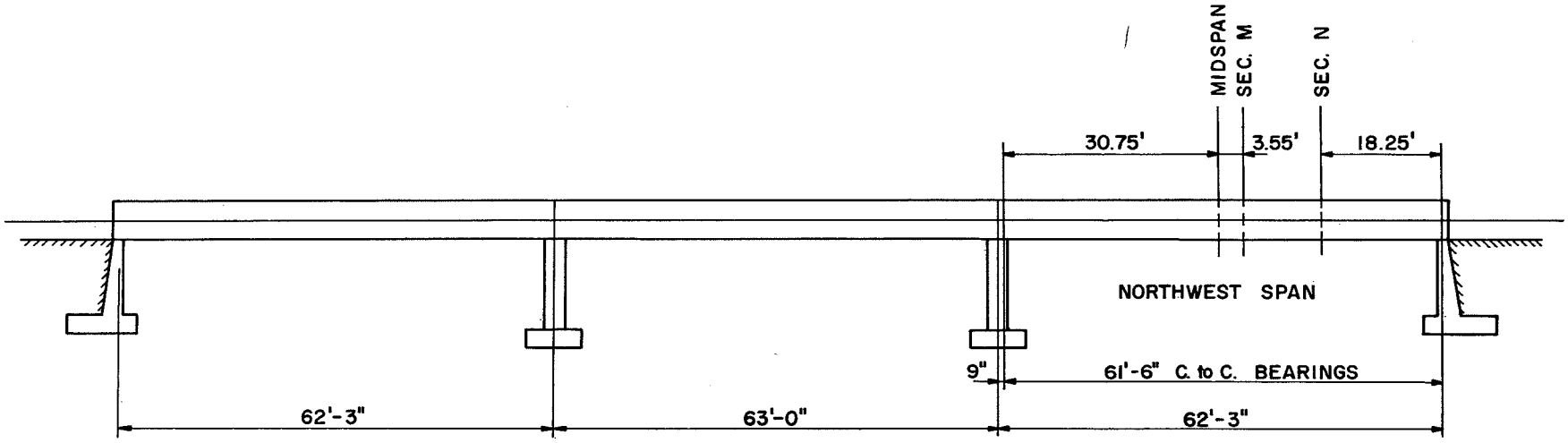

Fig. 1 Elevation of Box Girder Bridge

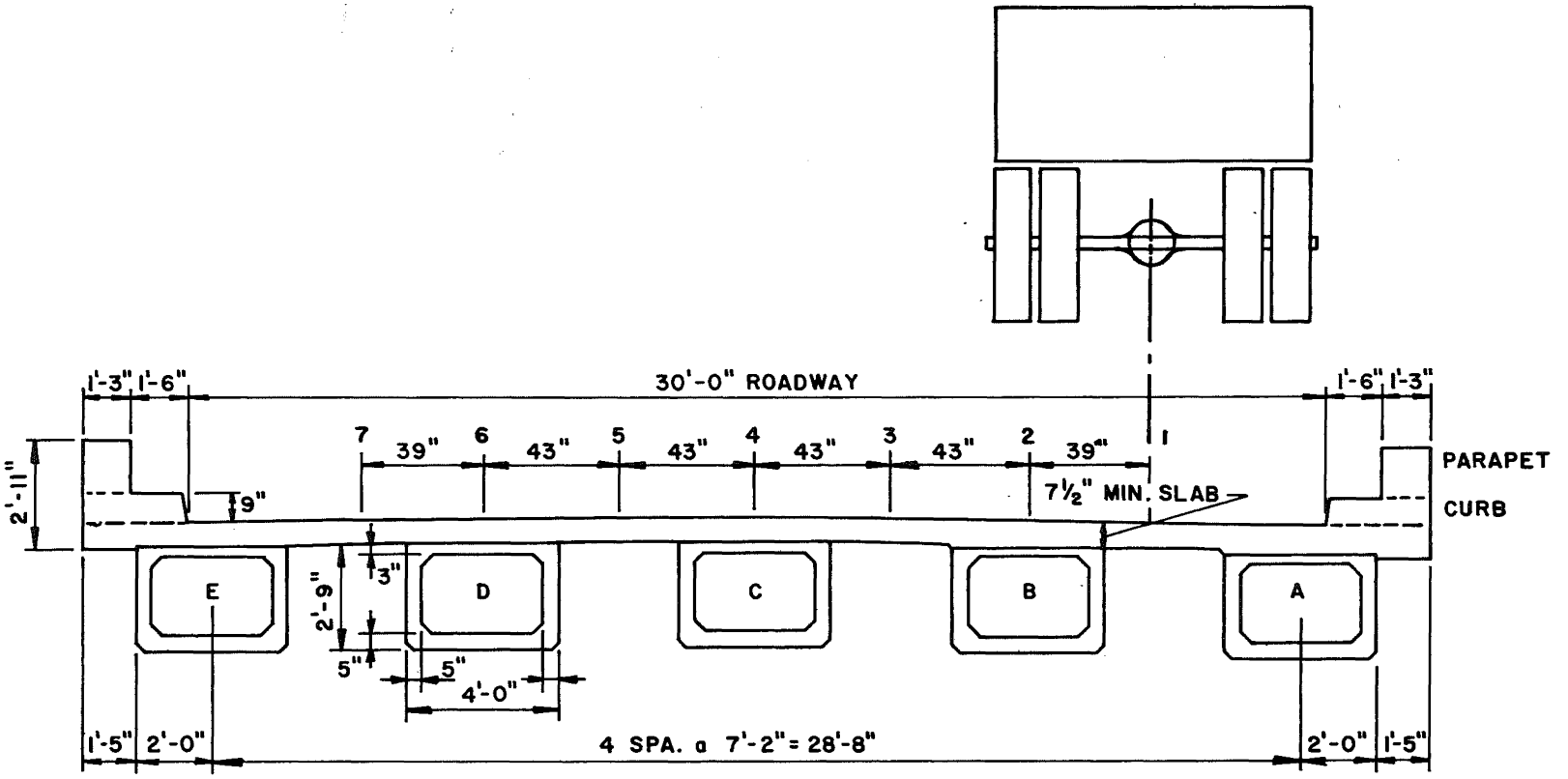

Fig. 2 Cross Section of Box Girder Bridge

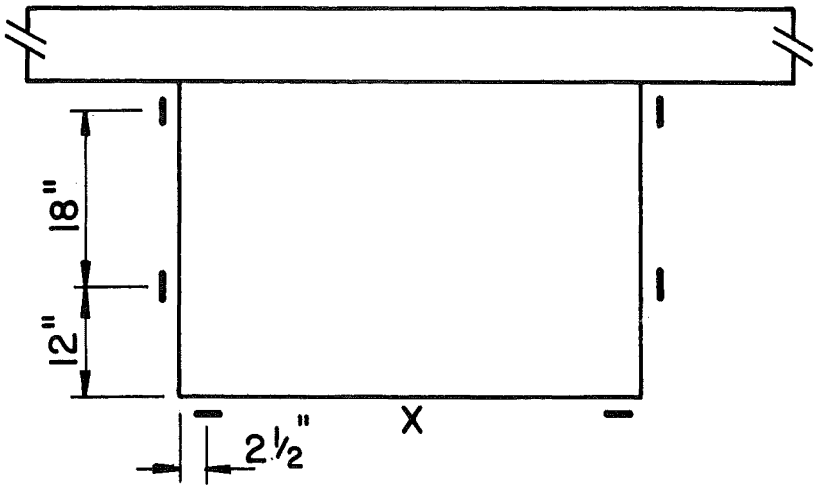

Gage Section M

Type of Gage	Symbol
Strain	—
Deflection	X

Fig. 3a Gage Location at Section M

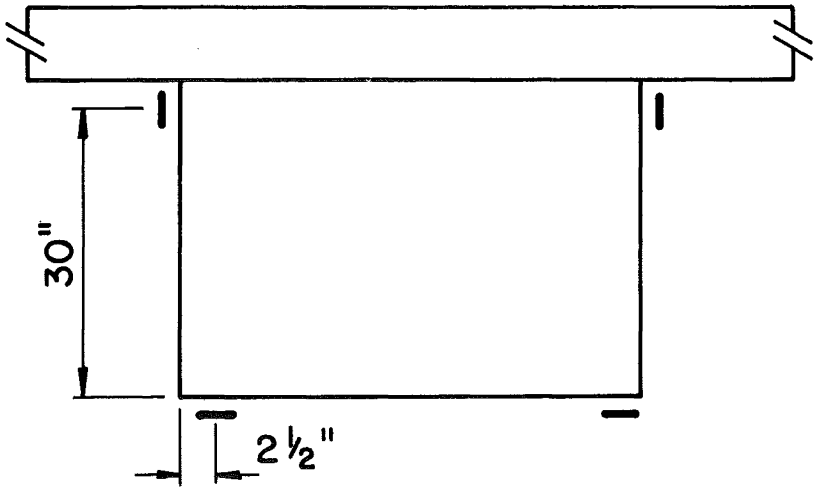

Gage Section N

Fig. 3b Gage Location at Section N

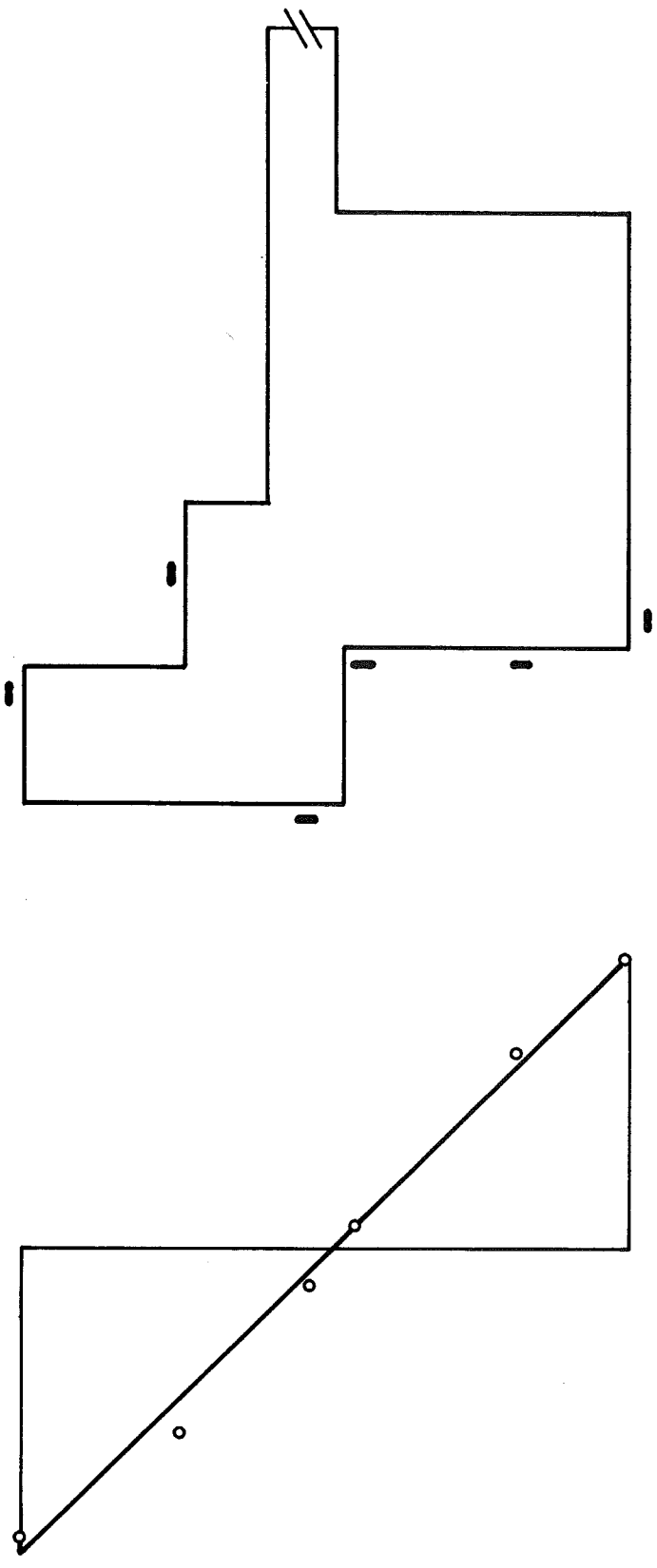

Fig. 4 Typical Strain Distribution at Outer Face of Exterior Girder E

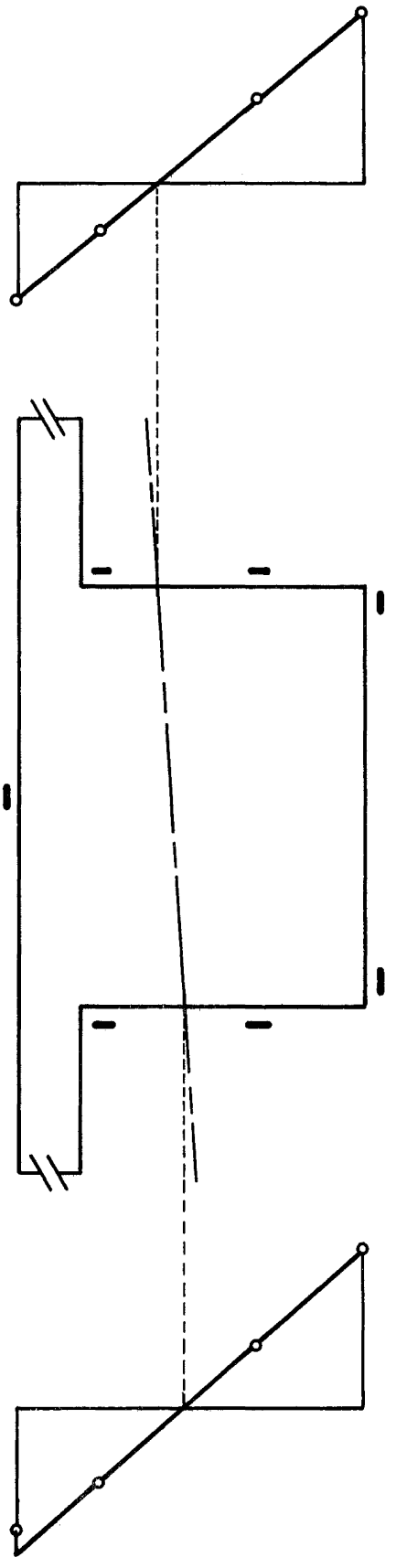

Fig. 5 Typical Strain Distribution at Faces of Interior Girder C

Fig. 6 Two-Truck Crawl Run

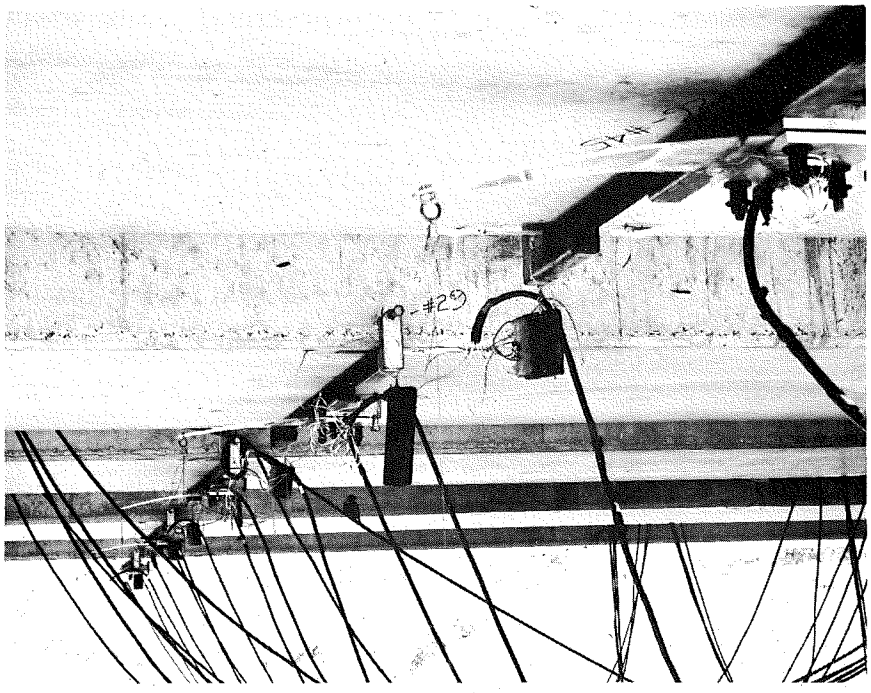

Fig. 7 Deflectometers

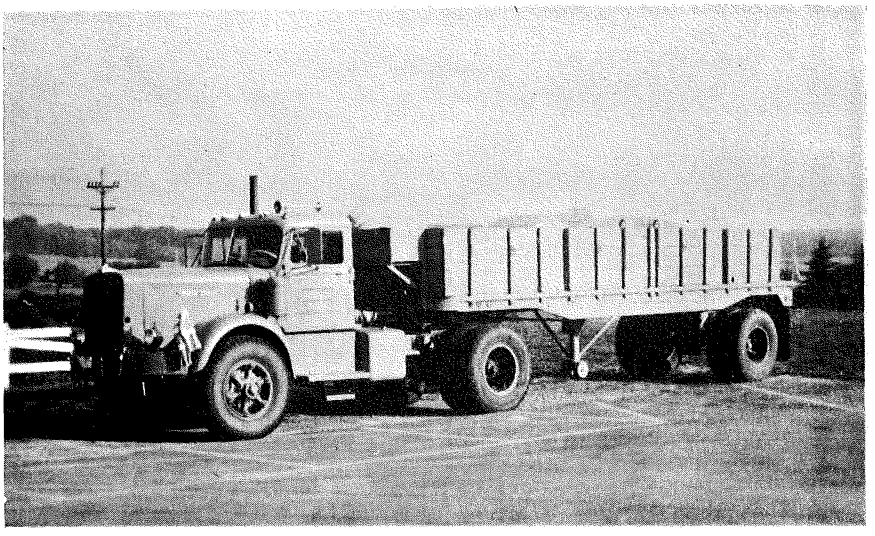

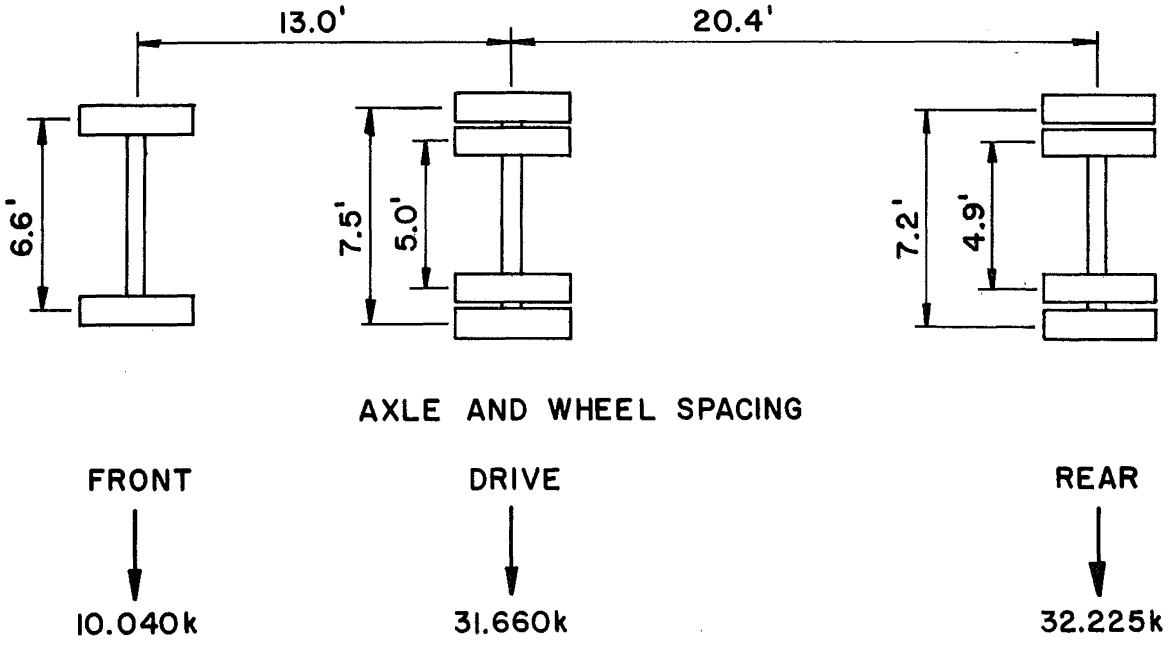

Fig. 8 Test Vehicle, T1

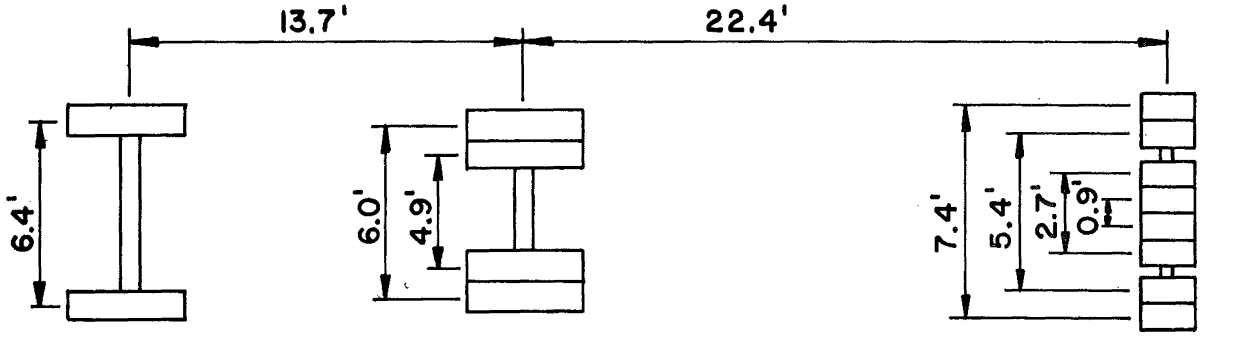

AXLE AND WHEEL SPACING

FRONT	DRIVE	REAR
9.260k	31.838k	32.600k

AXLE LOADS

Fig. 9 Test Vehicle, T2

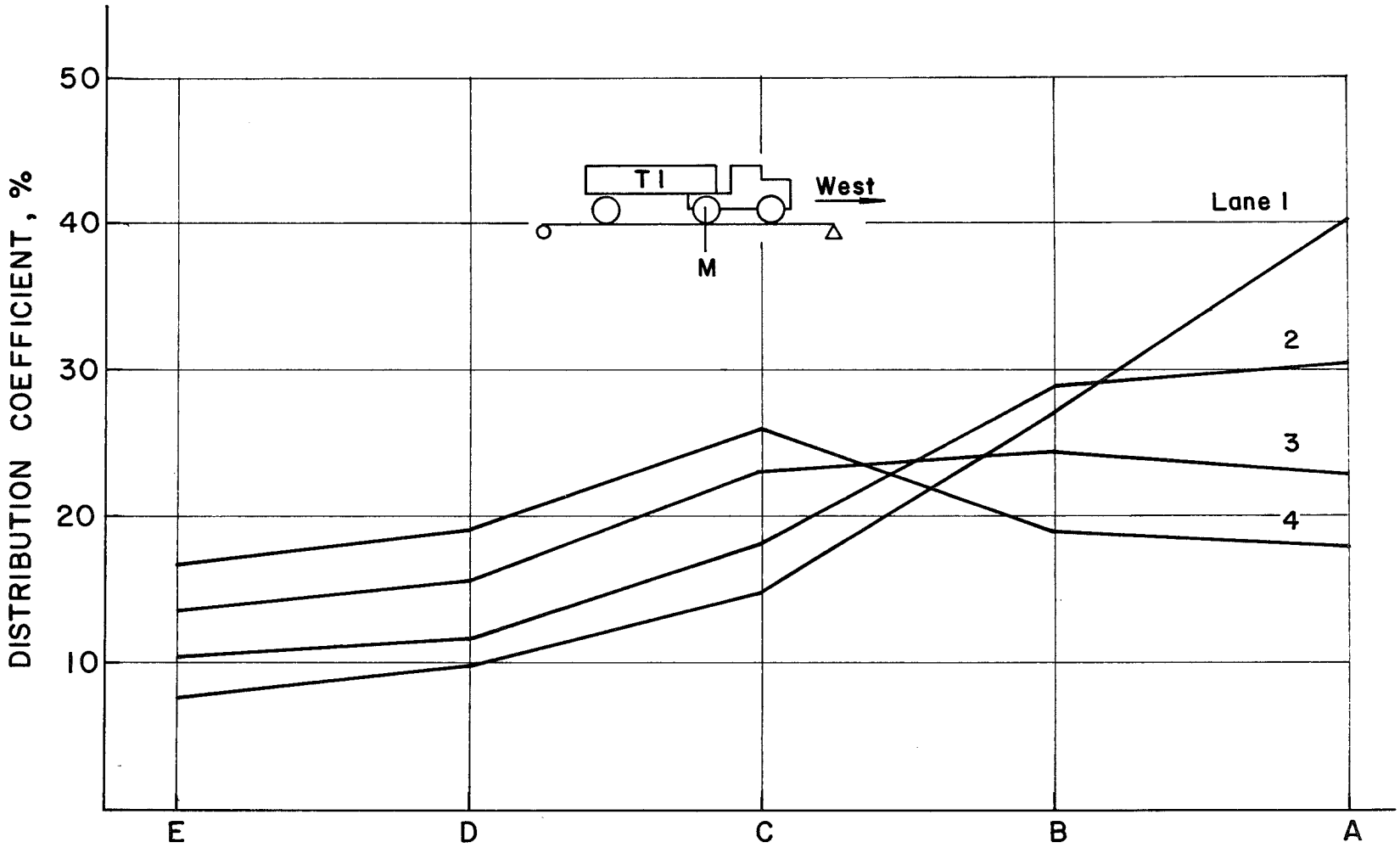

Fig. 10 Distribution Coefficients at Section M, Series I (T1, Westbound)

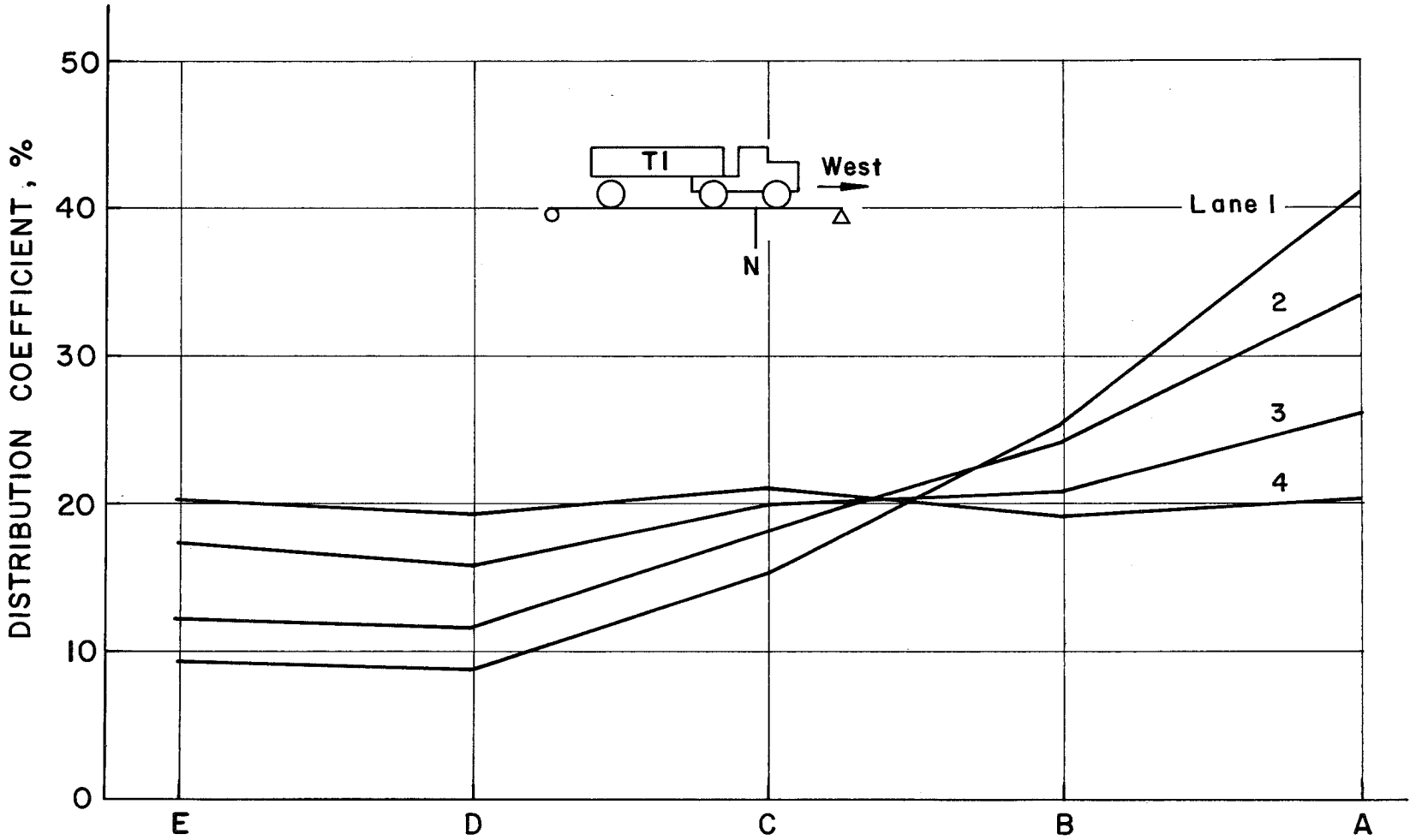

Fig. 11 Distribution Coefficients at Section N, Series I
(T1, Westbound)

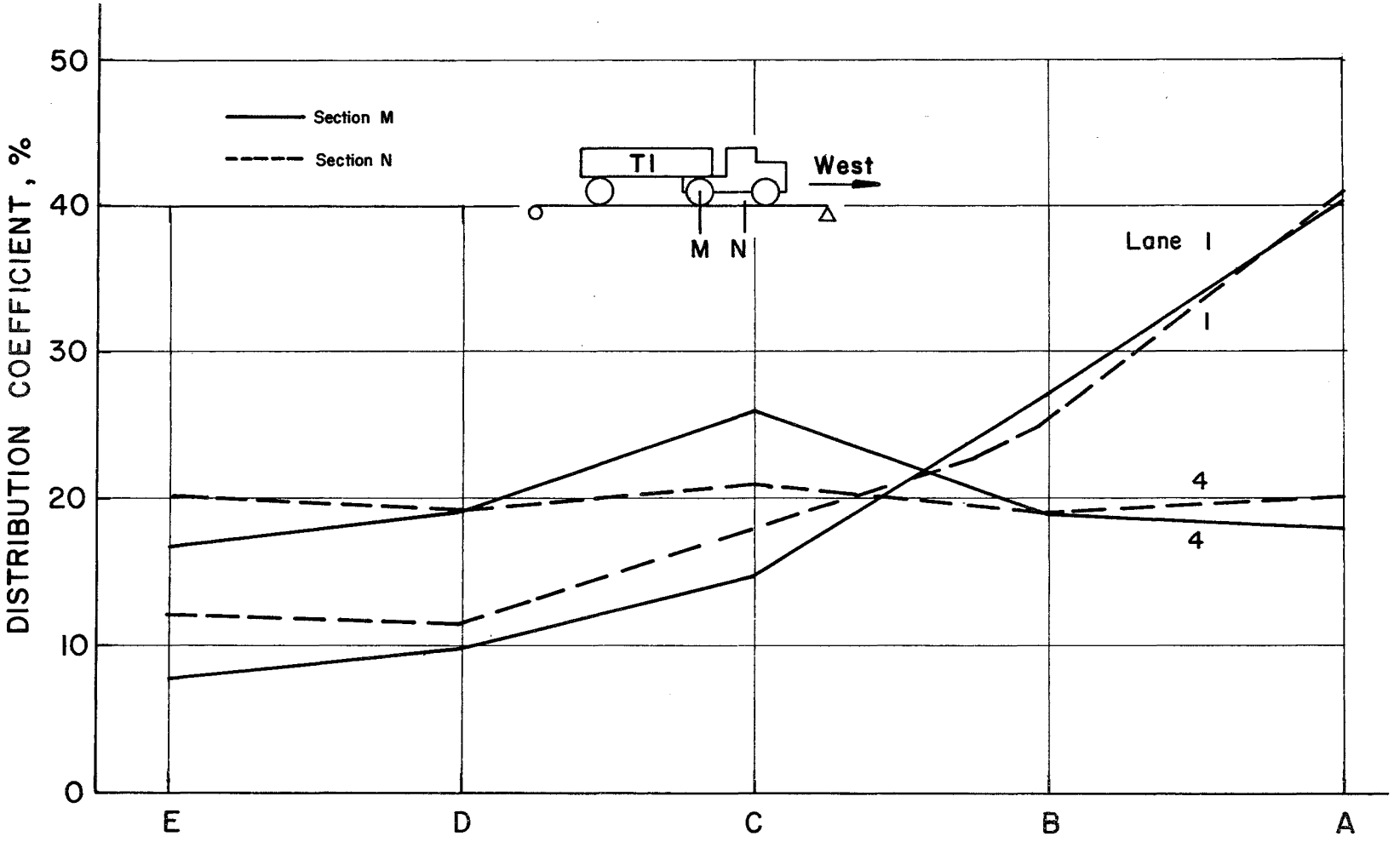

Fig. 12 Comparison of Distribution Coefficients at Sections M and N, Series I (T1, Westbound)

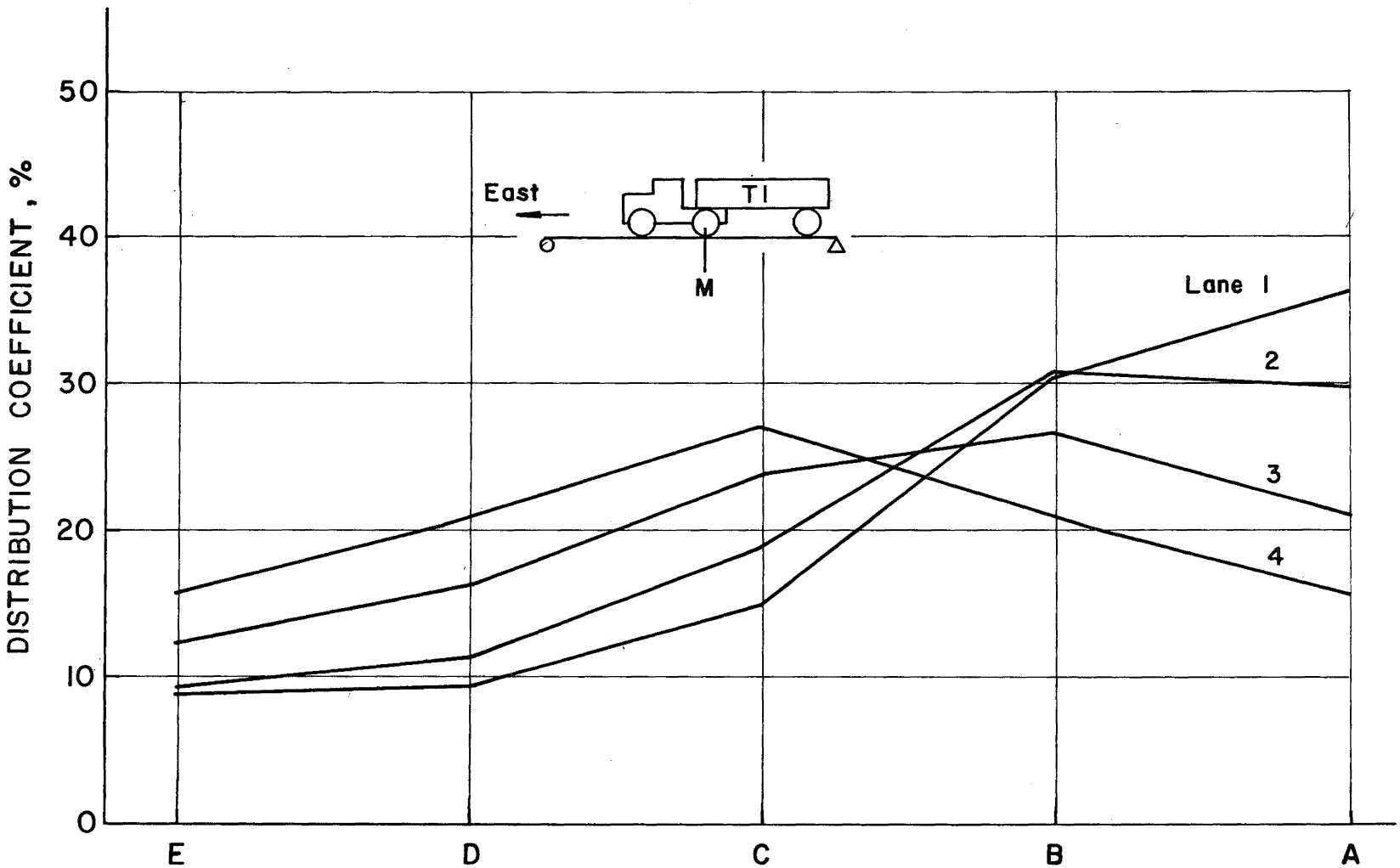

Fig. 13 Distribution Coefficients at Section M, Series I
(T1, Eastbound)

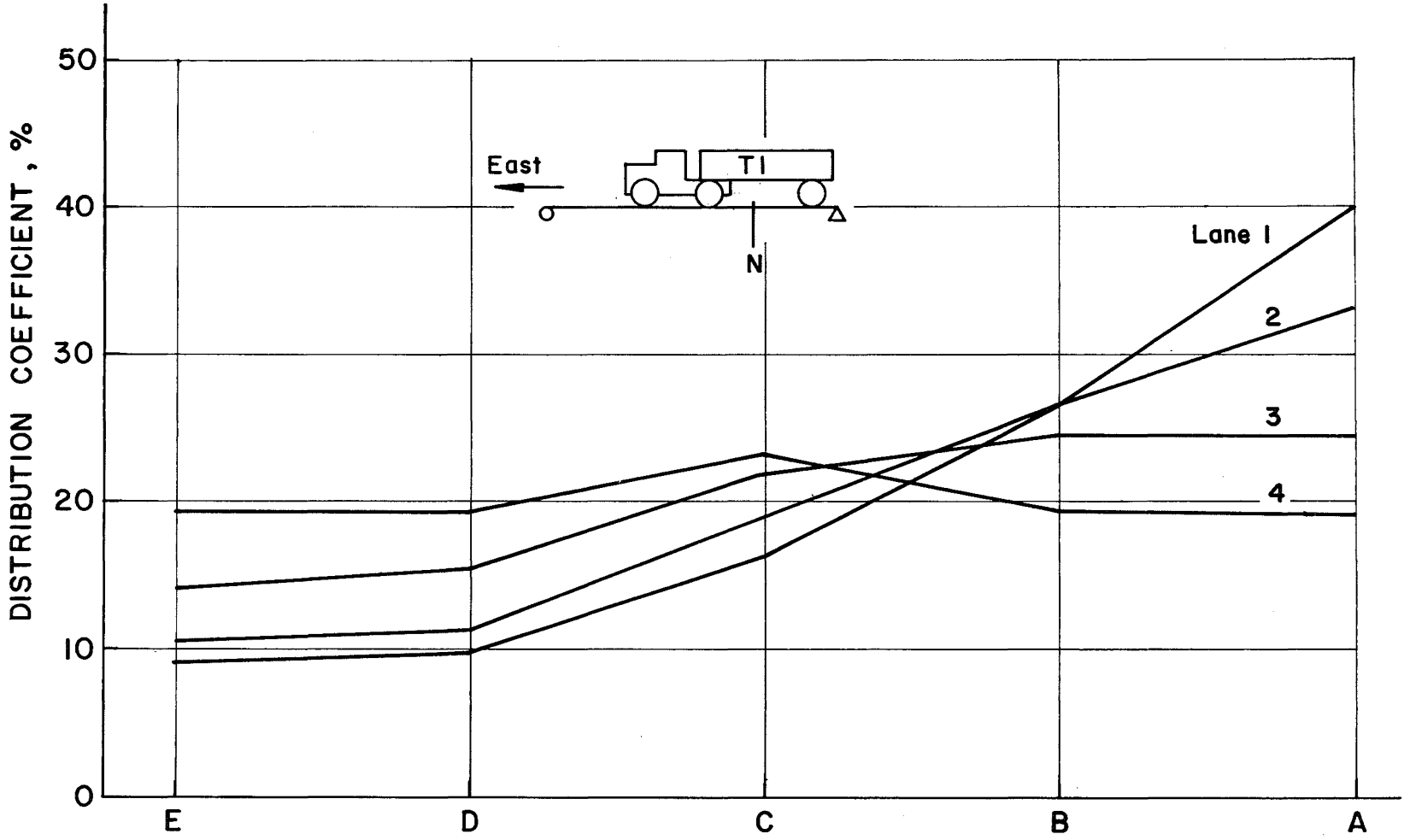

Fig. 14 Distribution Coefficients at Section N, Series I (T1, Eastbound)

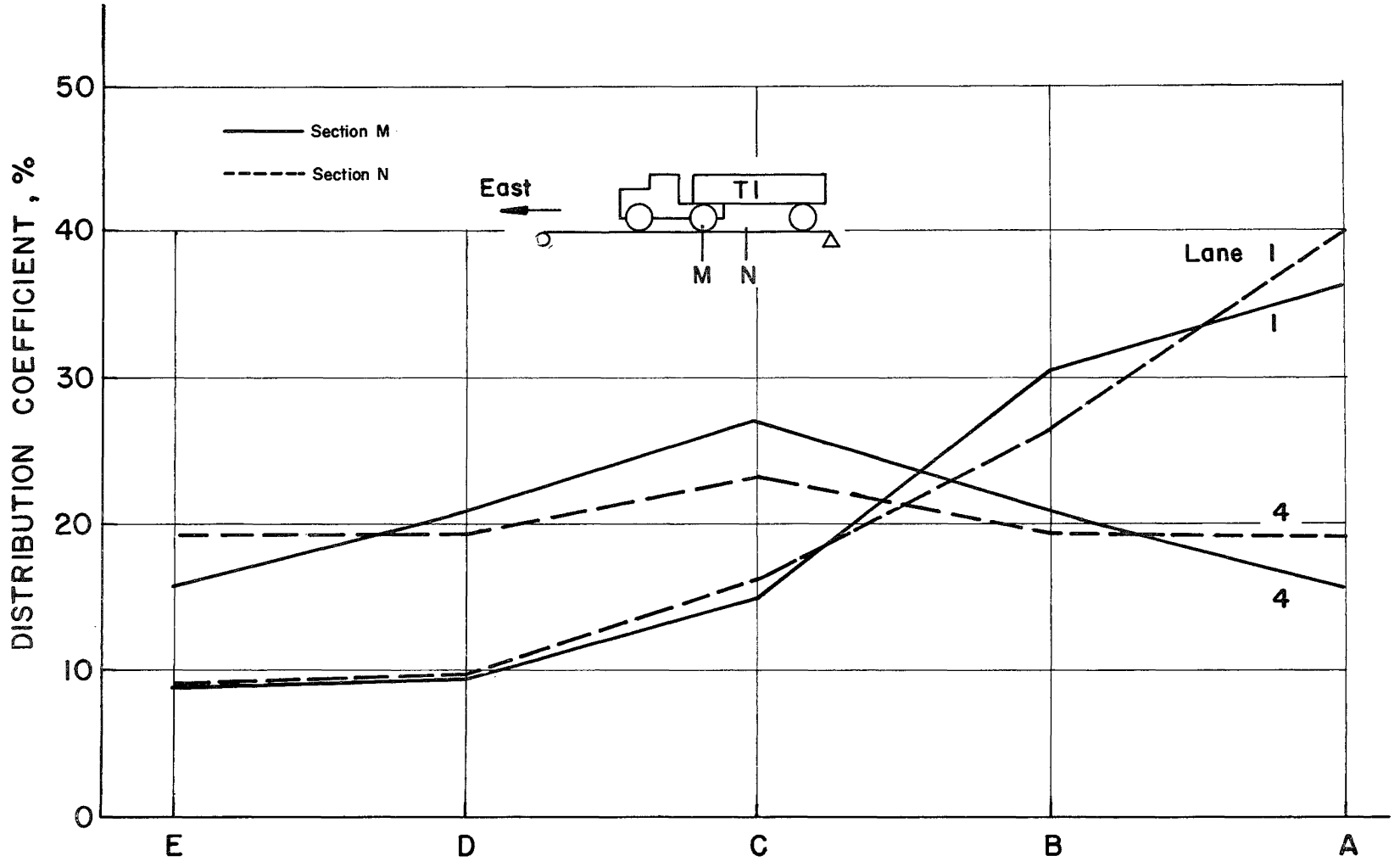

Fig. 15 Comparison of Distribution Coefficients at Sections M and N, Series I (T1, Eastbound)

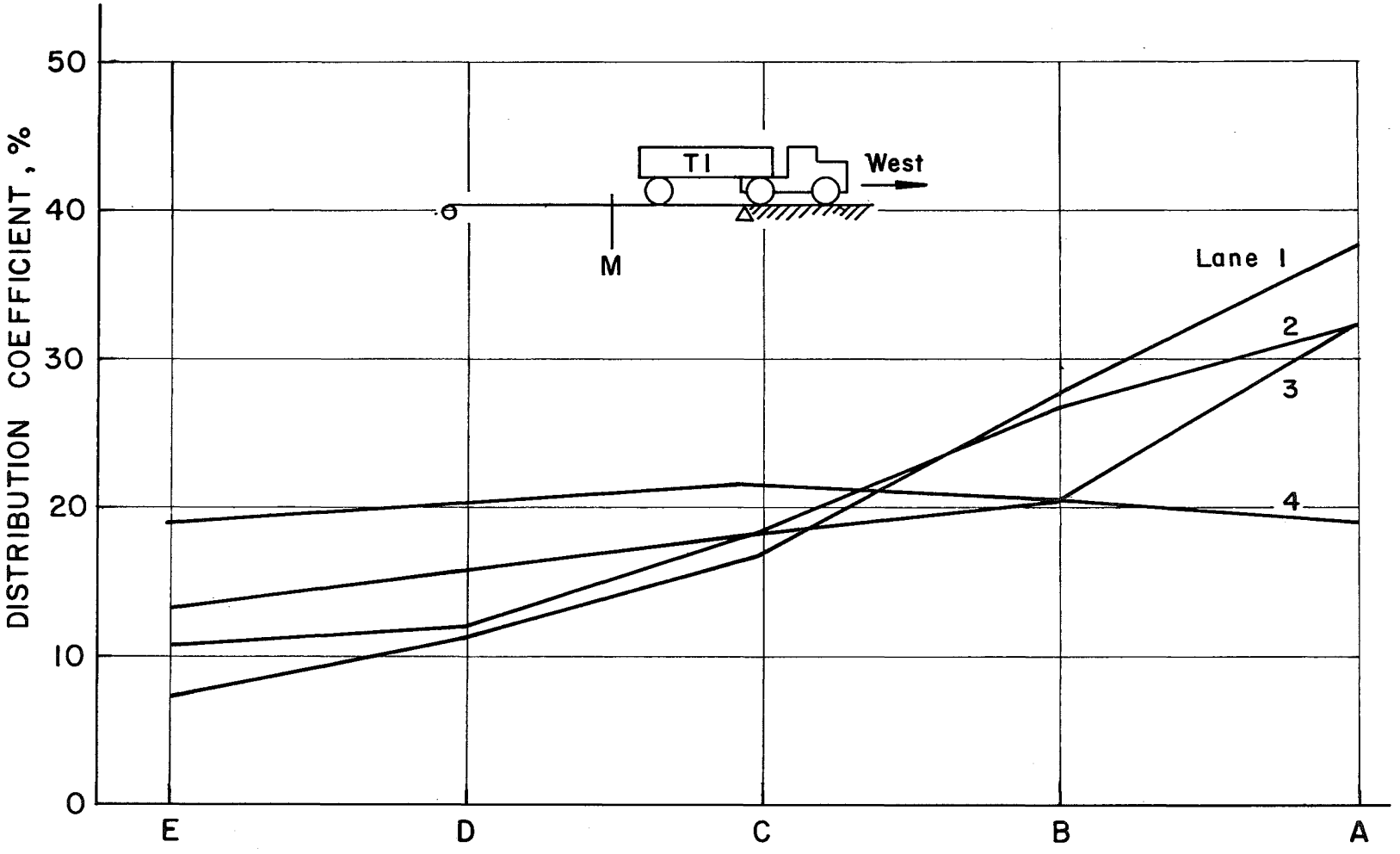

Fig. 16 Distribution Coefficients at Section M, Series I
(T1, Westbound, Single Axle Loading)

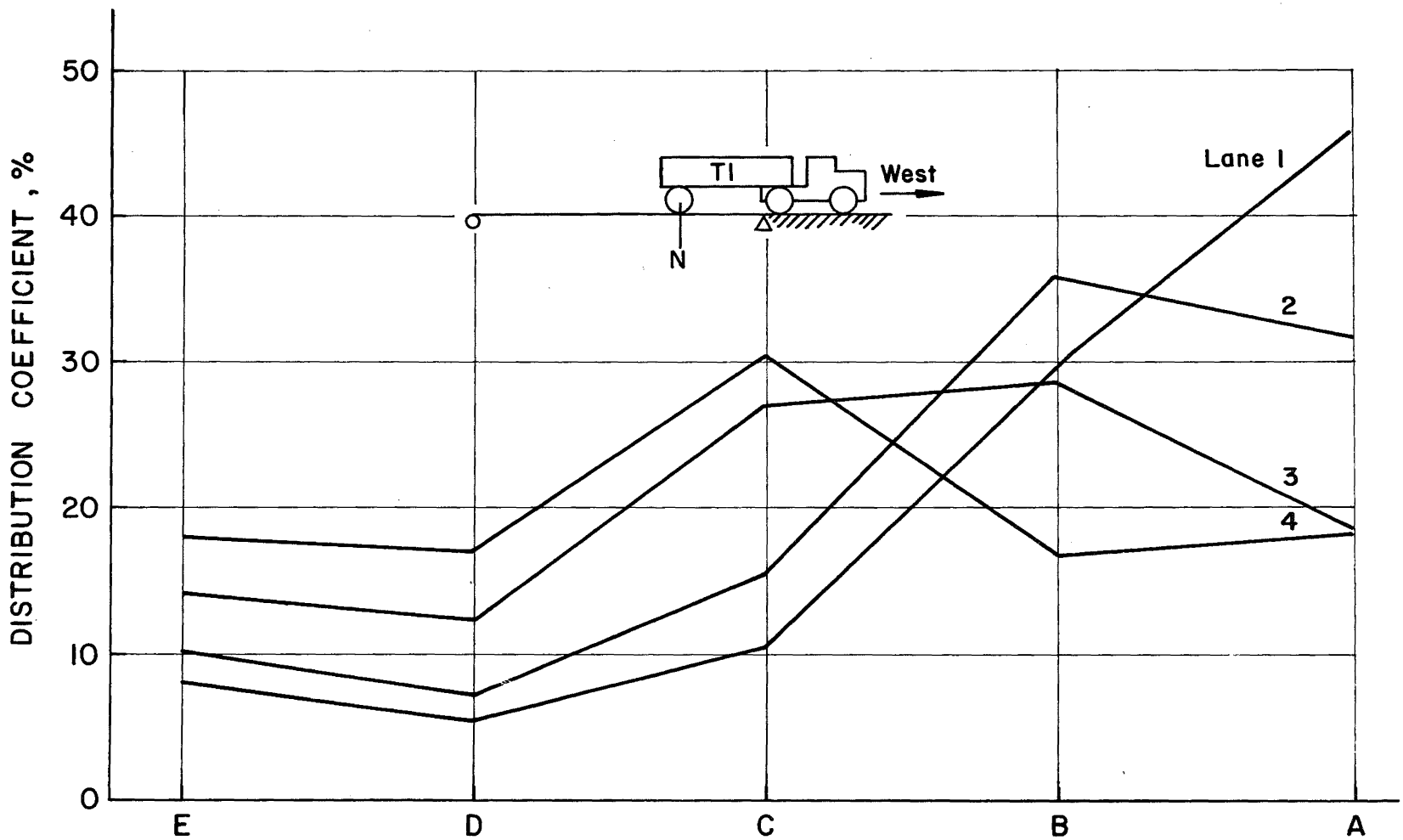

Fig. 17 Distribution Coefficients at Section N, Series I
(T1, Westbound, Single Axle Loading)

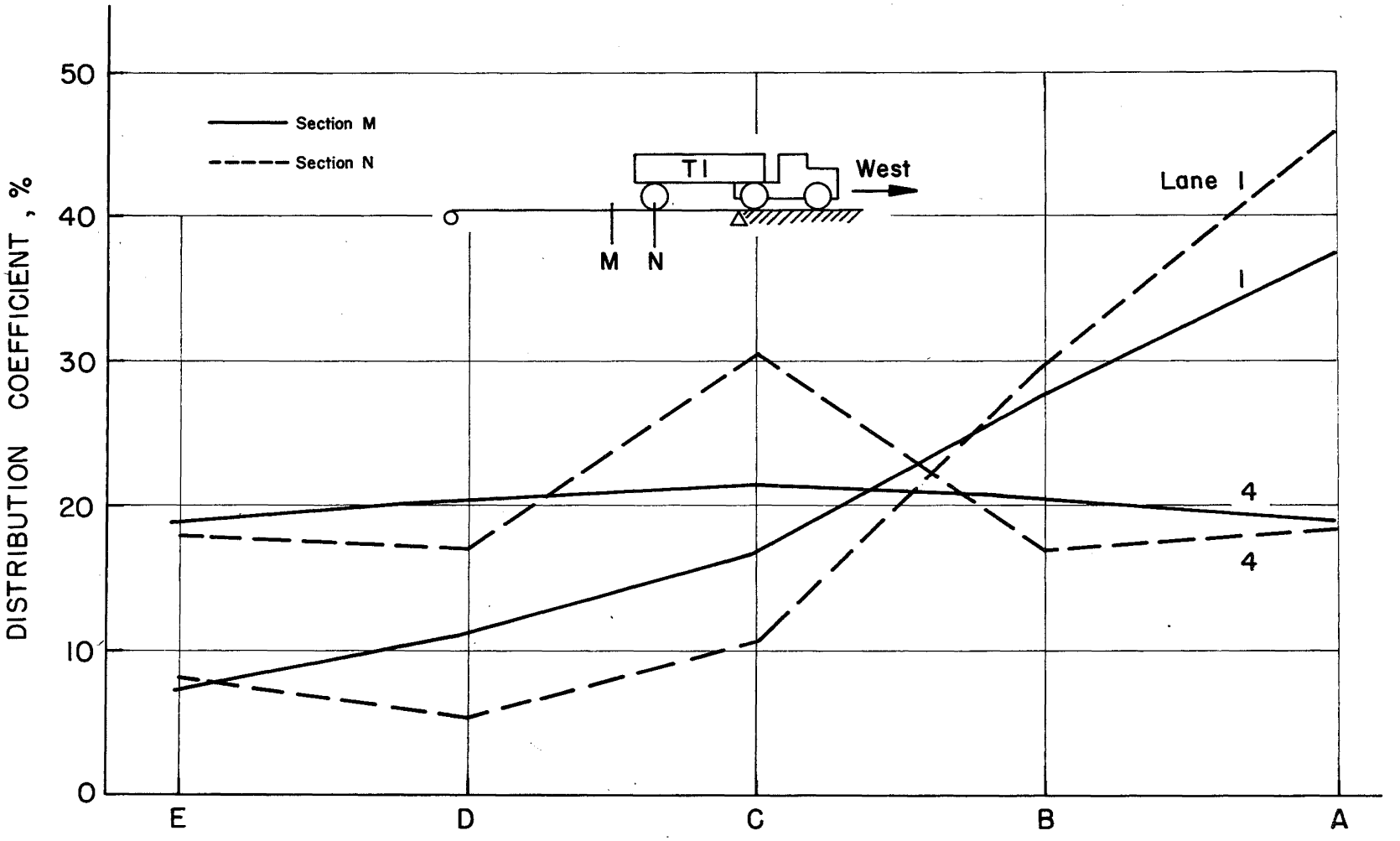

Fig. 18 Comparison of Distribution Coefficients at Sections M and N, Series I (T1, Westbound, Single Axle Loading)

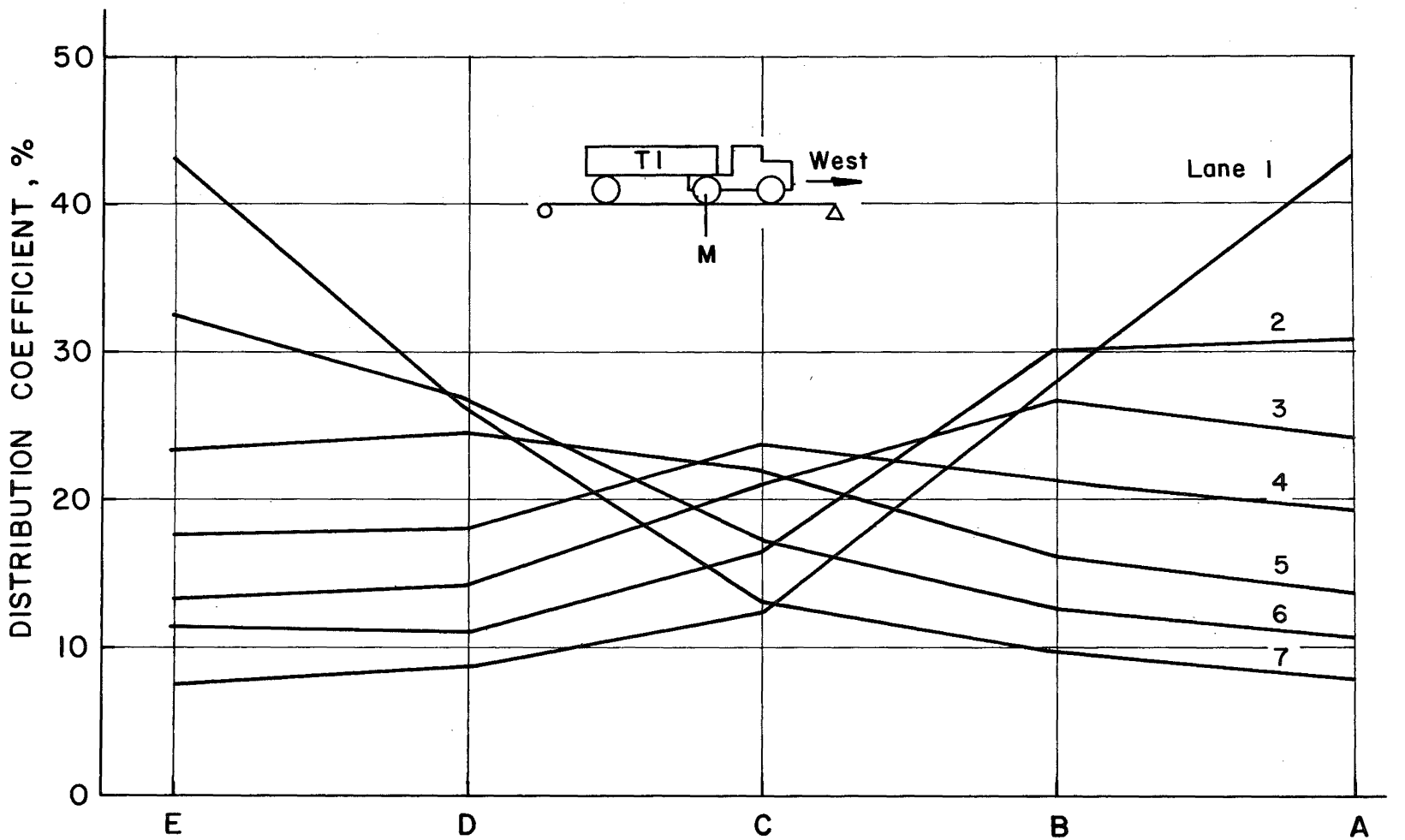

Fig. 19 Distribution Coefficients at Section M, Series II (T1, Westbound)

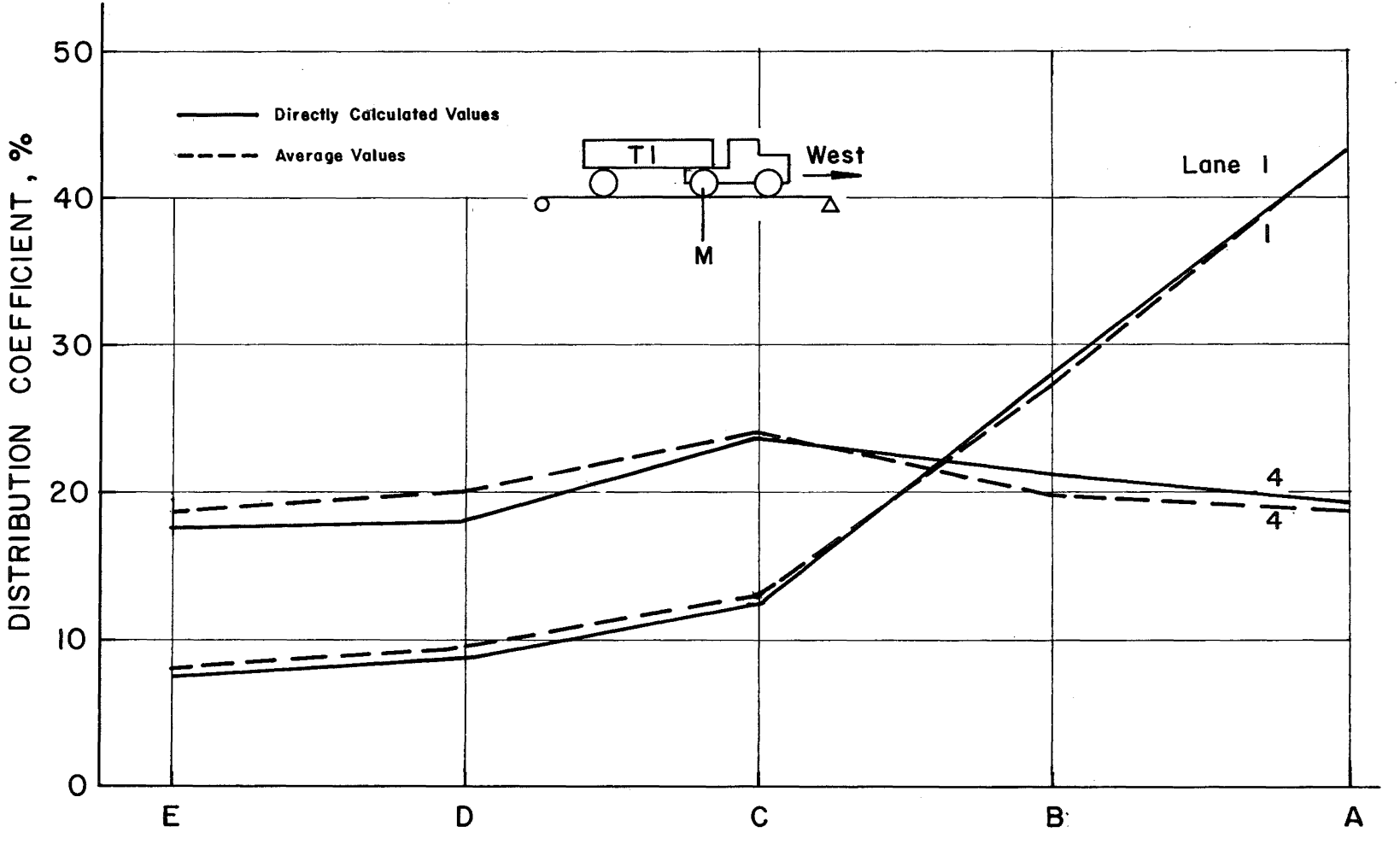

Fig. 20 Comparison of Distribution Coefficients at Section M, Series II (T1, Westbound)

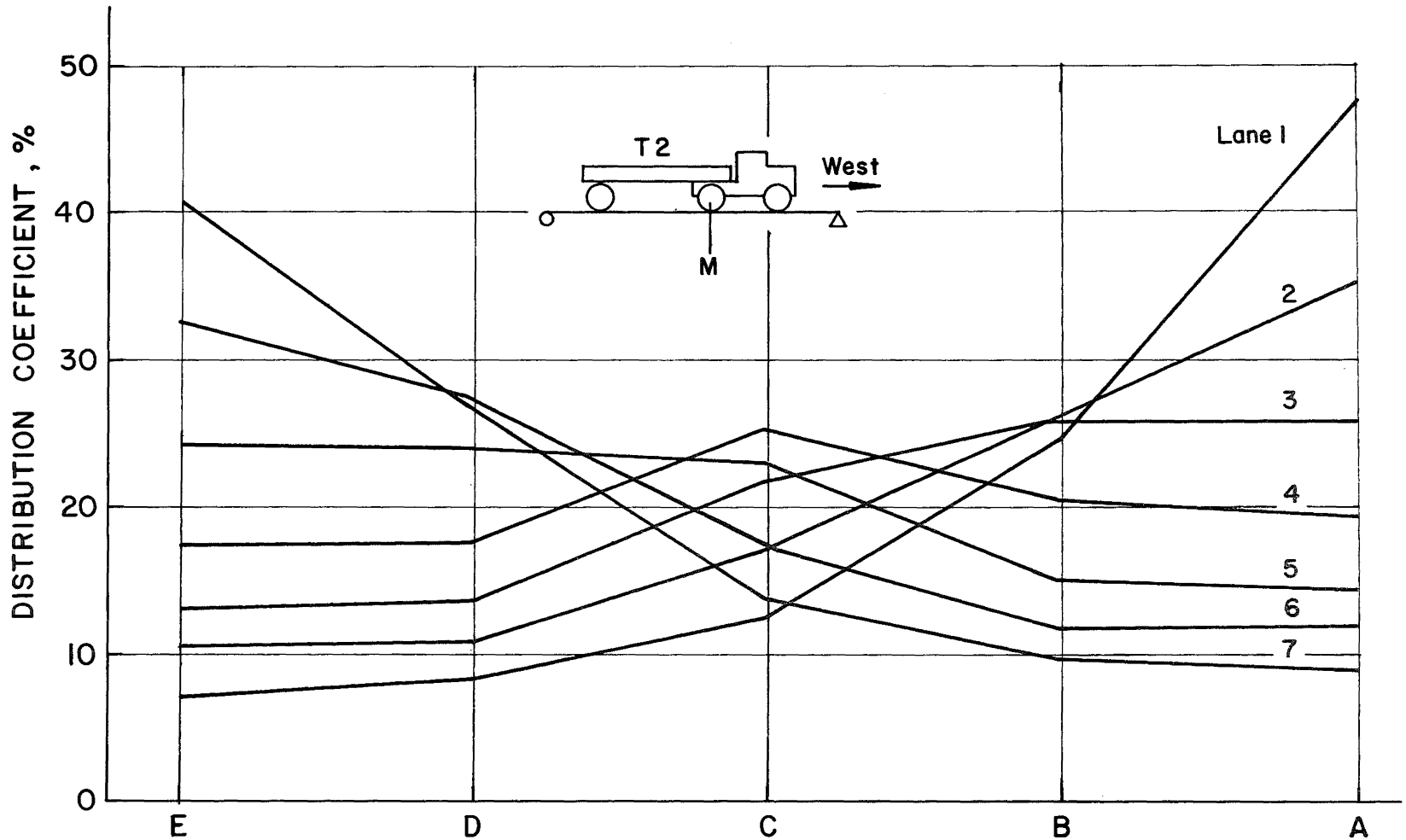

Fig. 21 Distribution Coefficients at Section M, Series II (T2, Westbound)

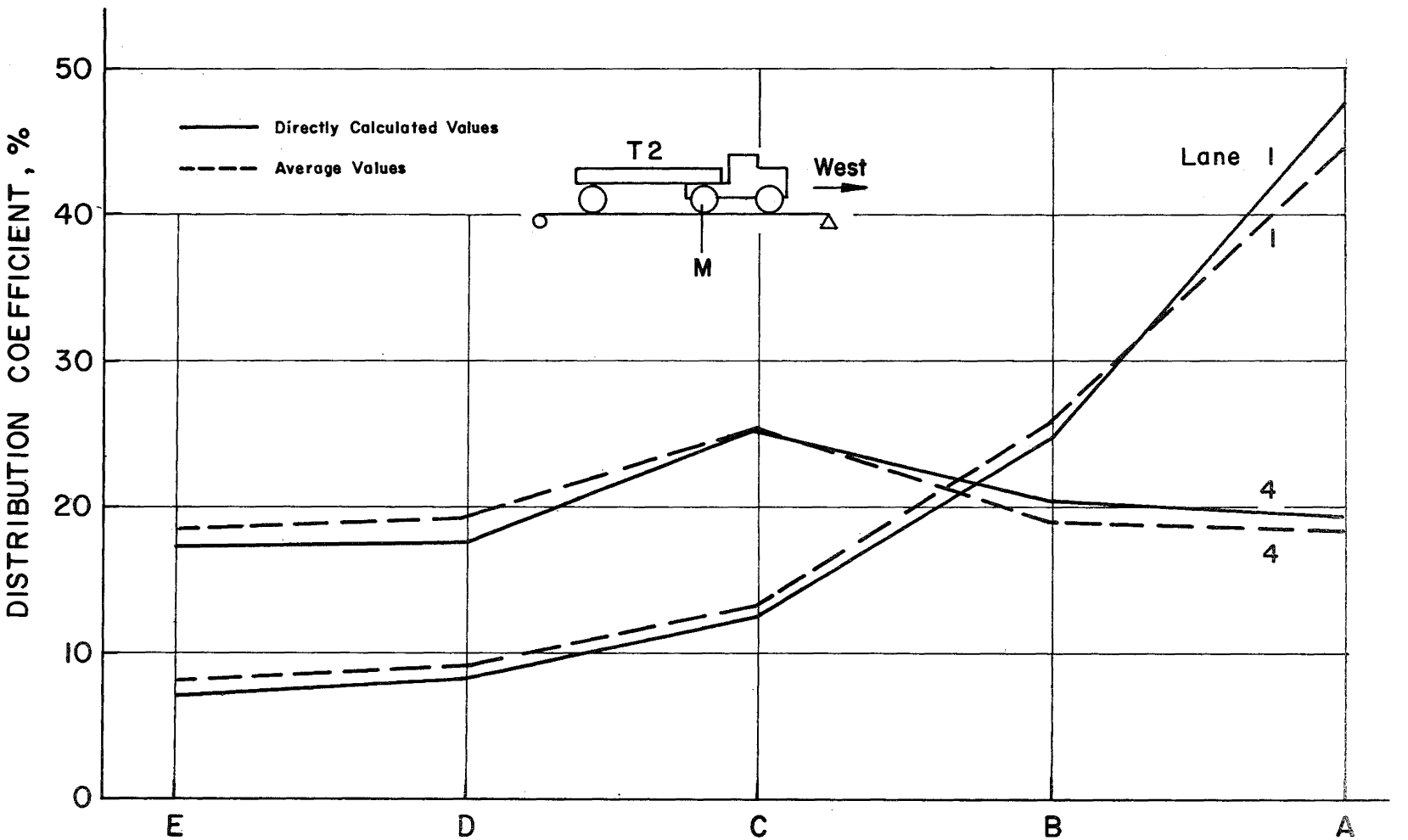

Fig. 22 Comparison of Distribution Coefficients at Section M, Series II (T2, Westbound)

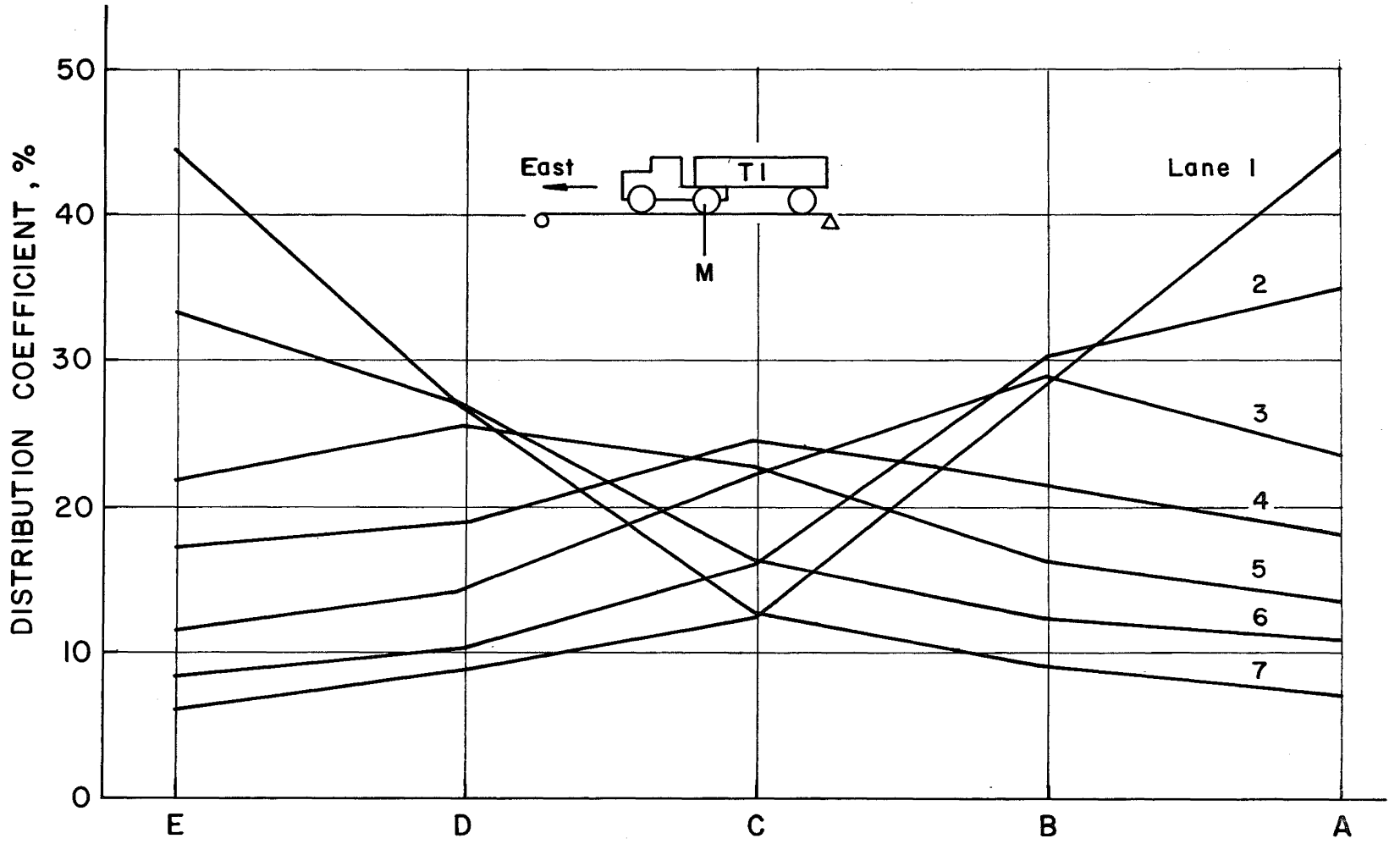

Fig. 23 Distribution Coefficients at Section M, Series II (T1, Eastbound)

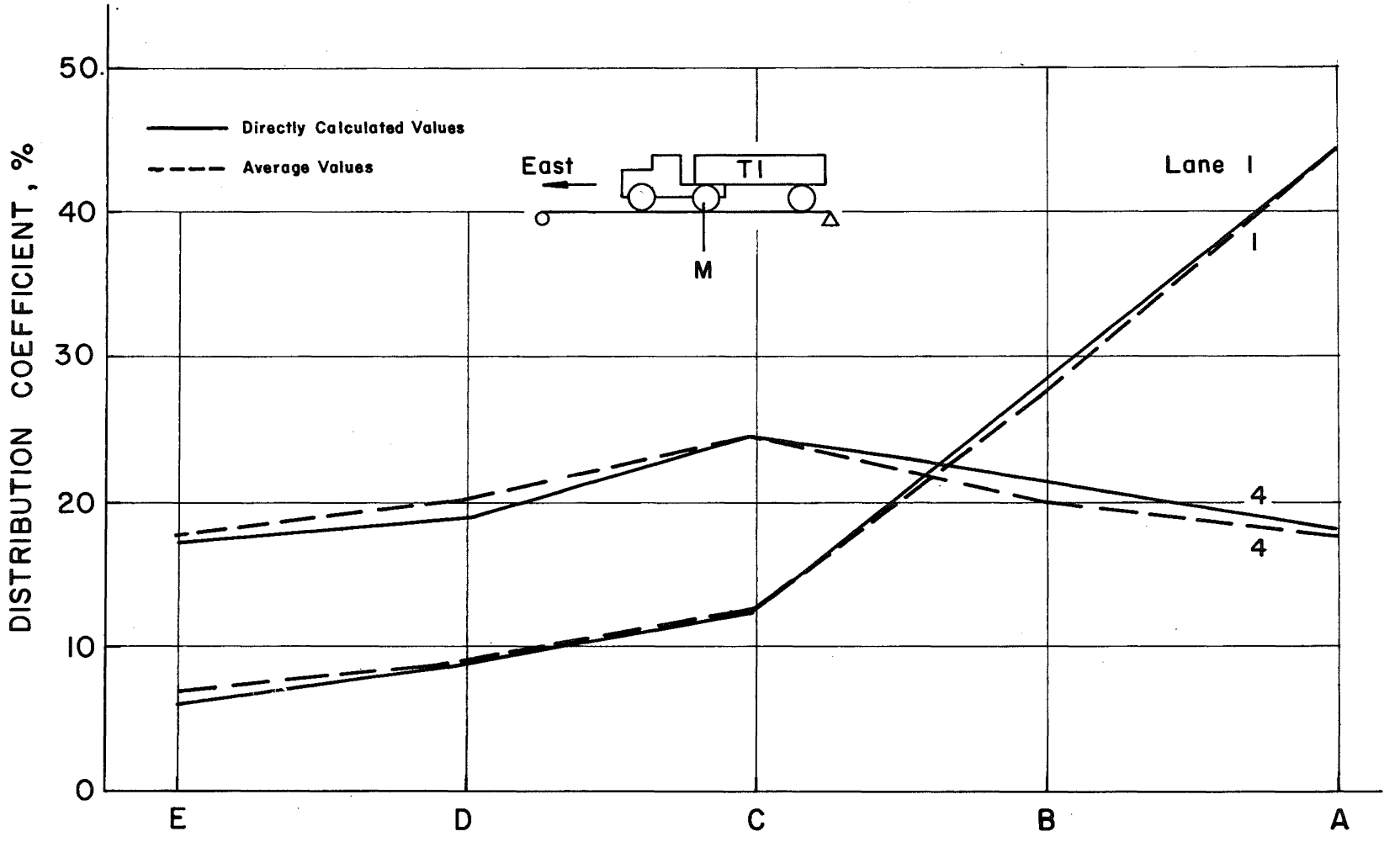

Fig. 24 Comparison of Distribution Coefficients at Section M, Series II (T1, Eastbound)

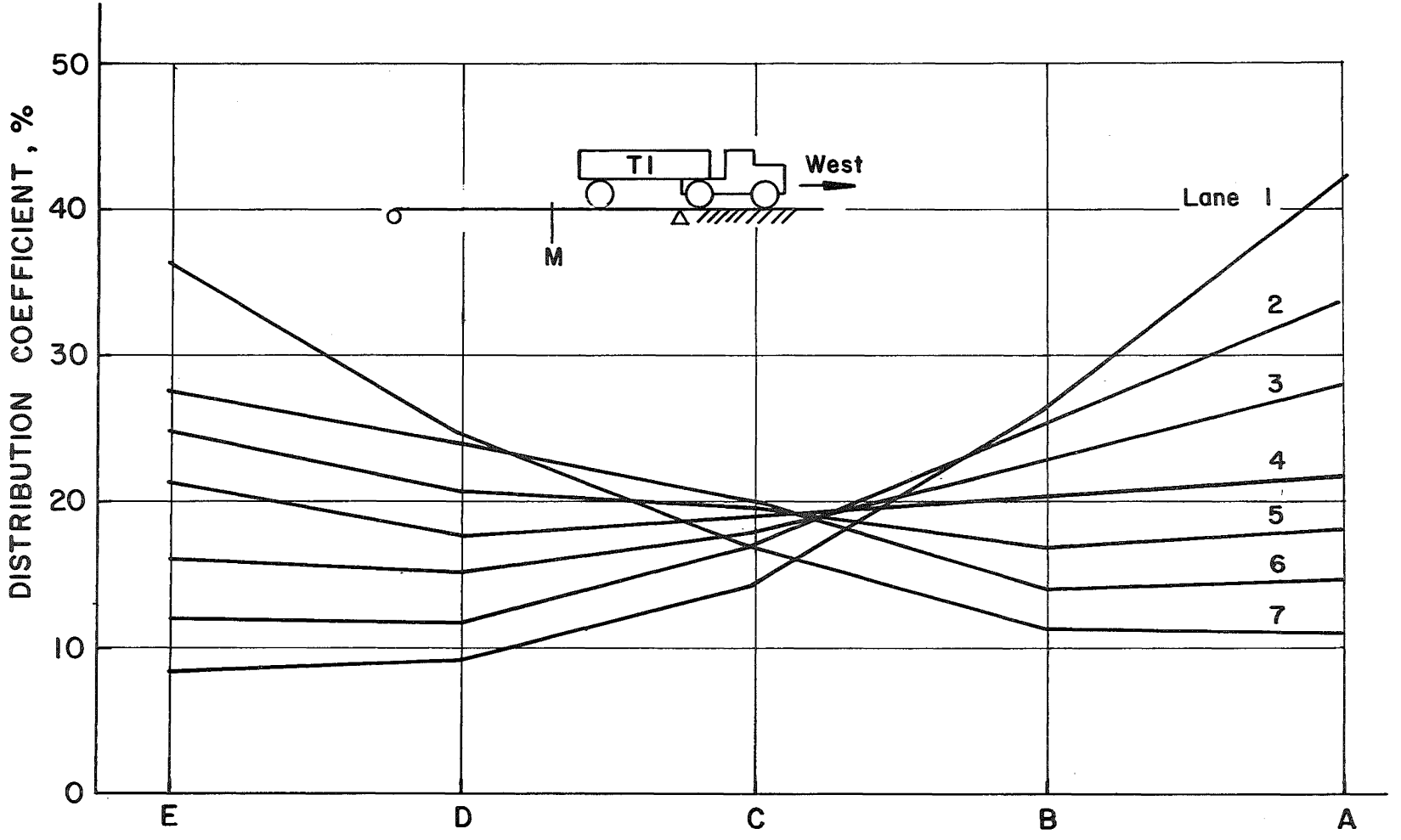

Fig. 25 Distribution Coefficients at Section M, Series II
(T1, Westbound, Single Axle Loading)

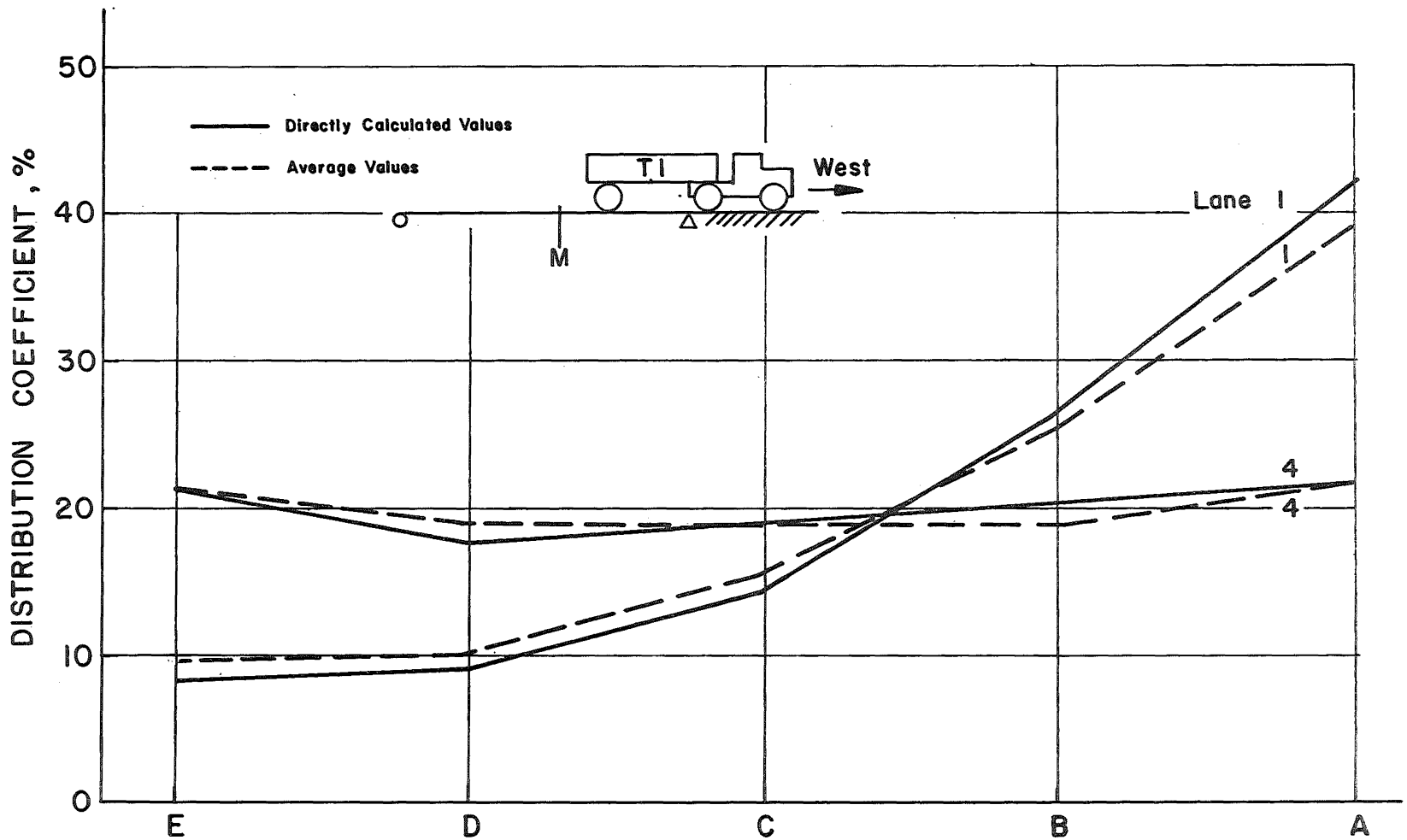

Fig. 26 Comparison of Distribution Coefficients at Section M, Series II (T1, Westbound, Single Axle Loading)

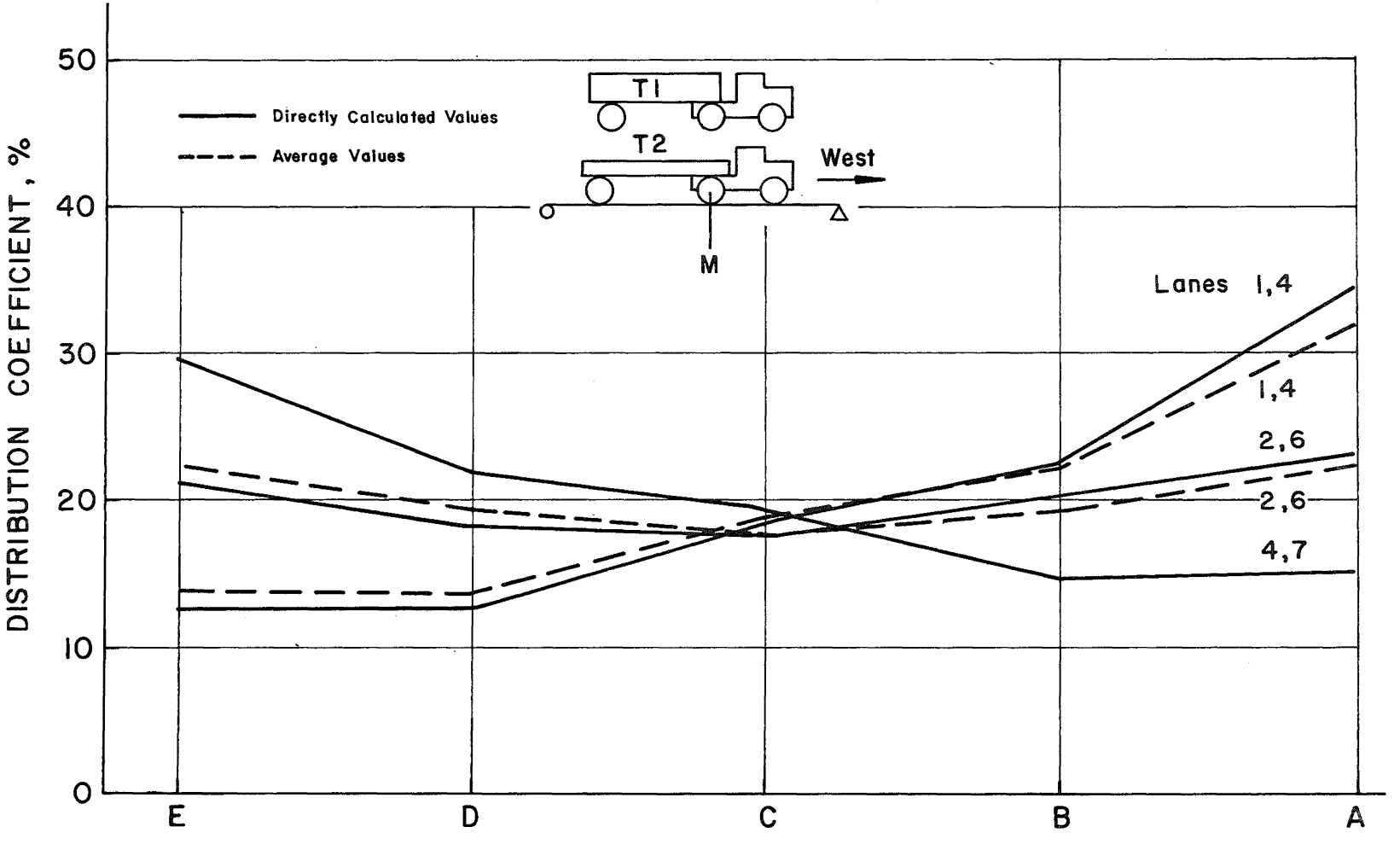

Fig. 27 Distribution Coefficients at Section M, Series II
(Two-Truck Runs, T1 and T2, Westbound)

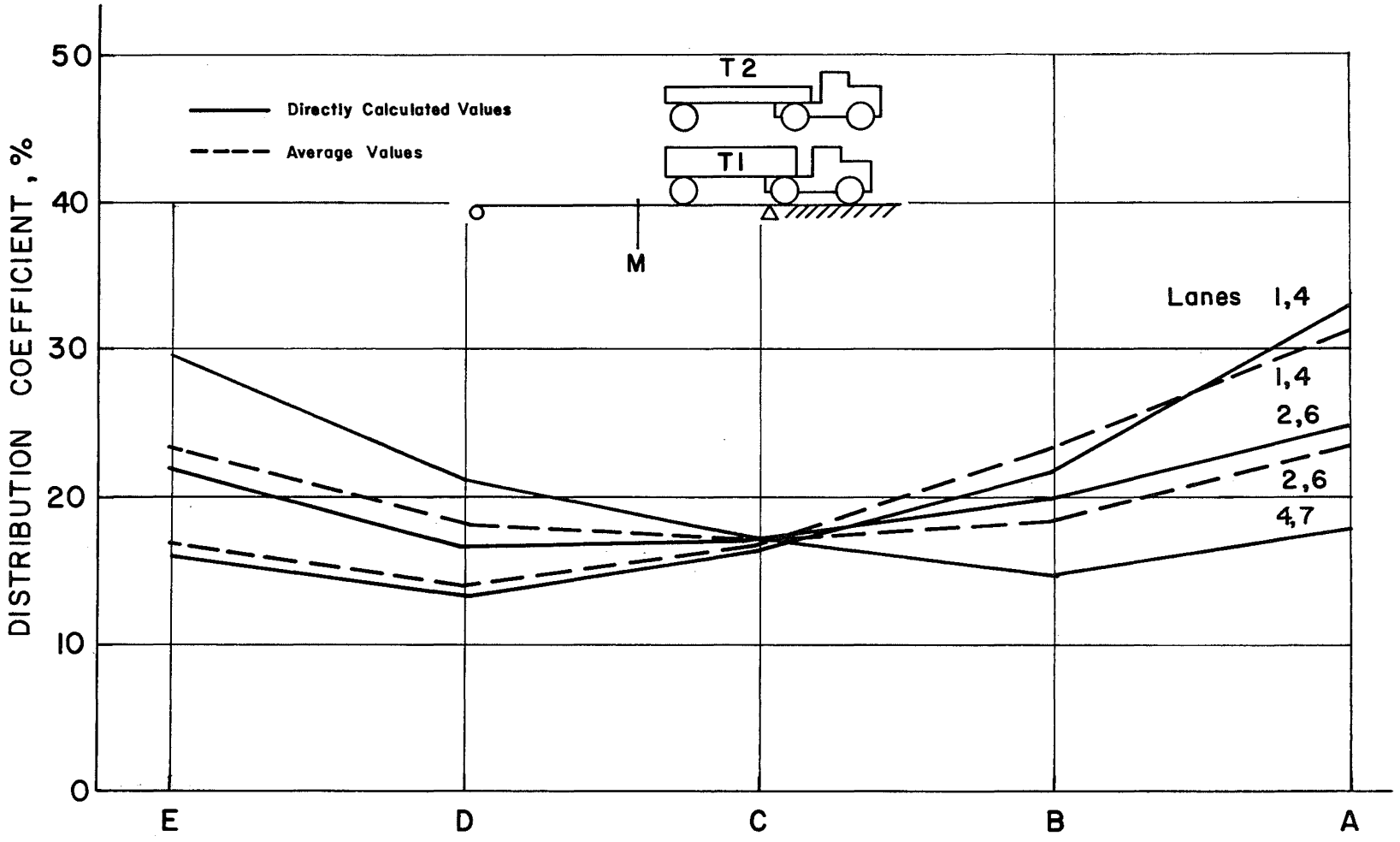

Fig. 28 Distribution Coefficients at Section M, Series II
(Two-Truck Runs, T1 and T2, Westbound)

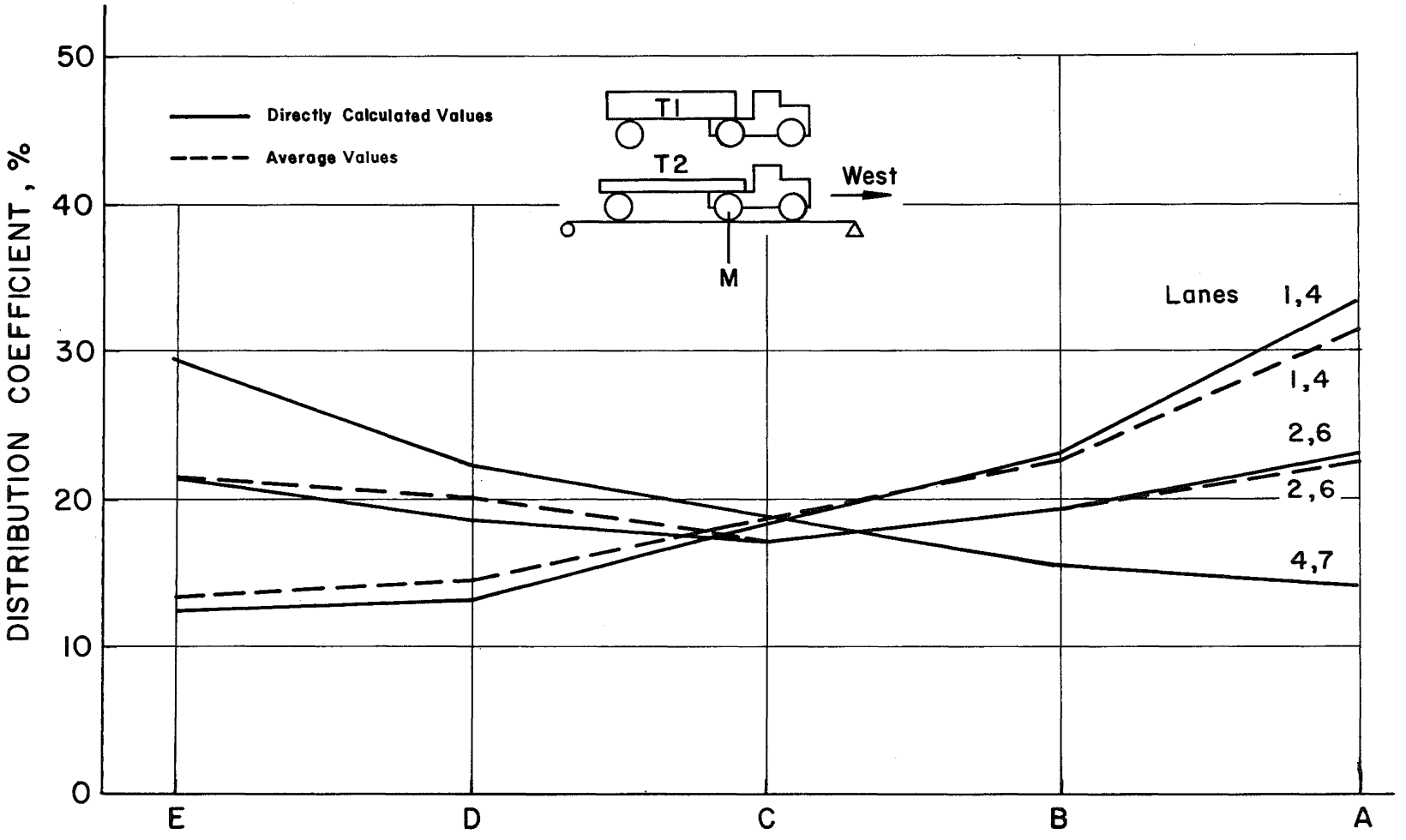

Fig. 29 Distribution Coefficients at Section M, Series II
(Superimposed Single-Truck Runs, T1 and T2, Westbound)

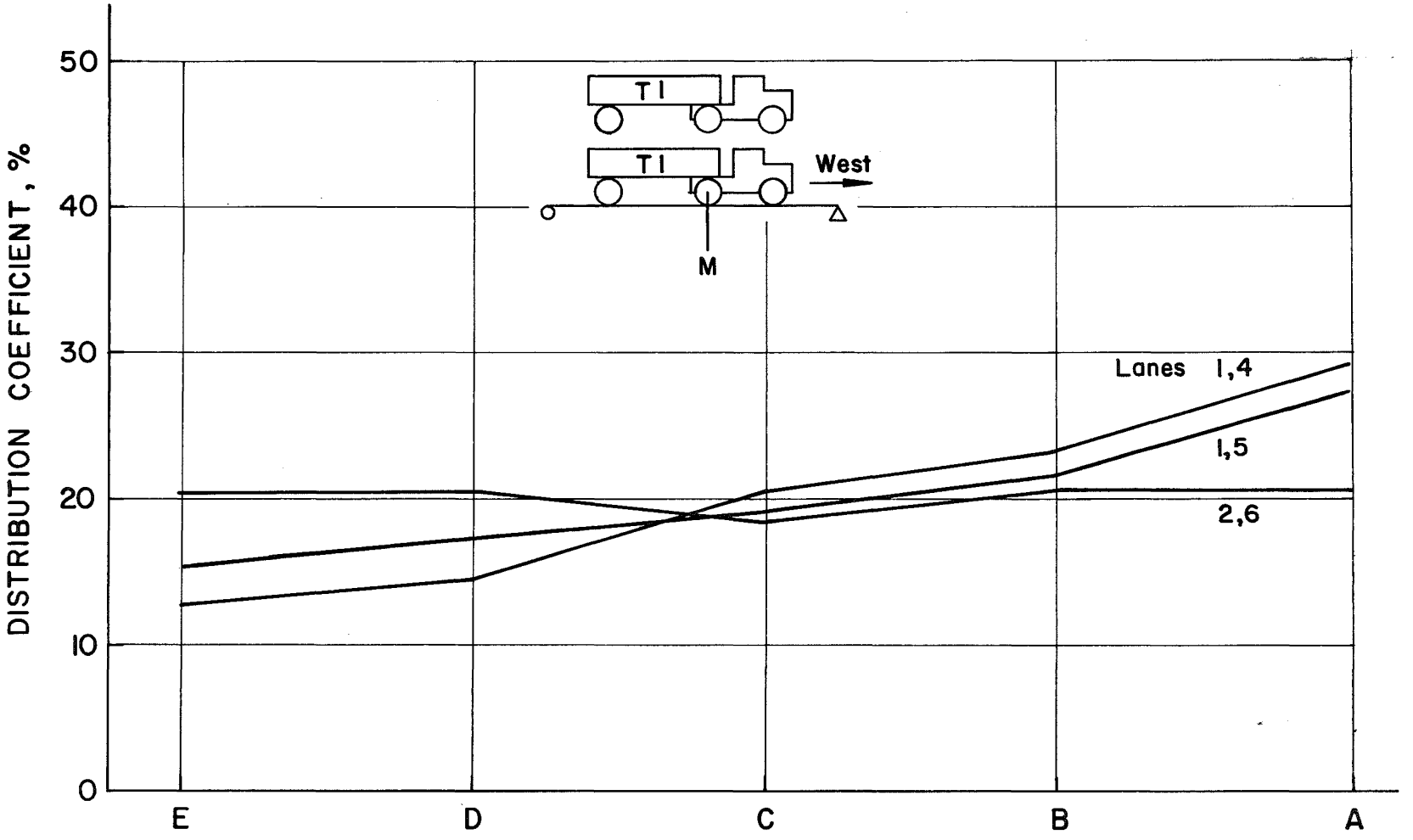

Fig. 30 Distribution Coefficients at Section M, Series I
(Superimposed Single-Truck Runs, T1 and T1, Westbound)

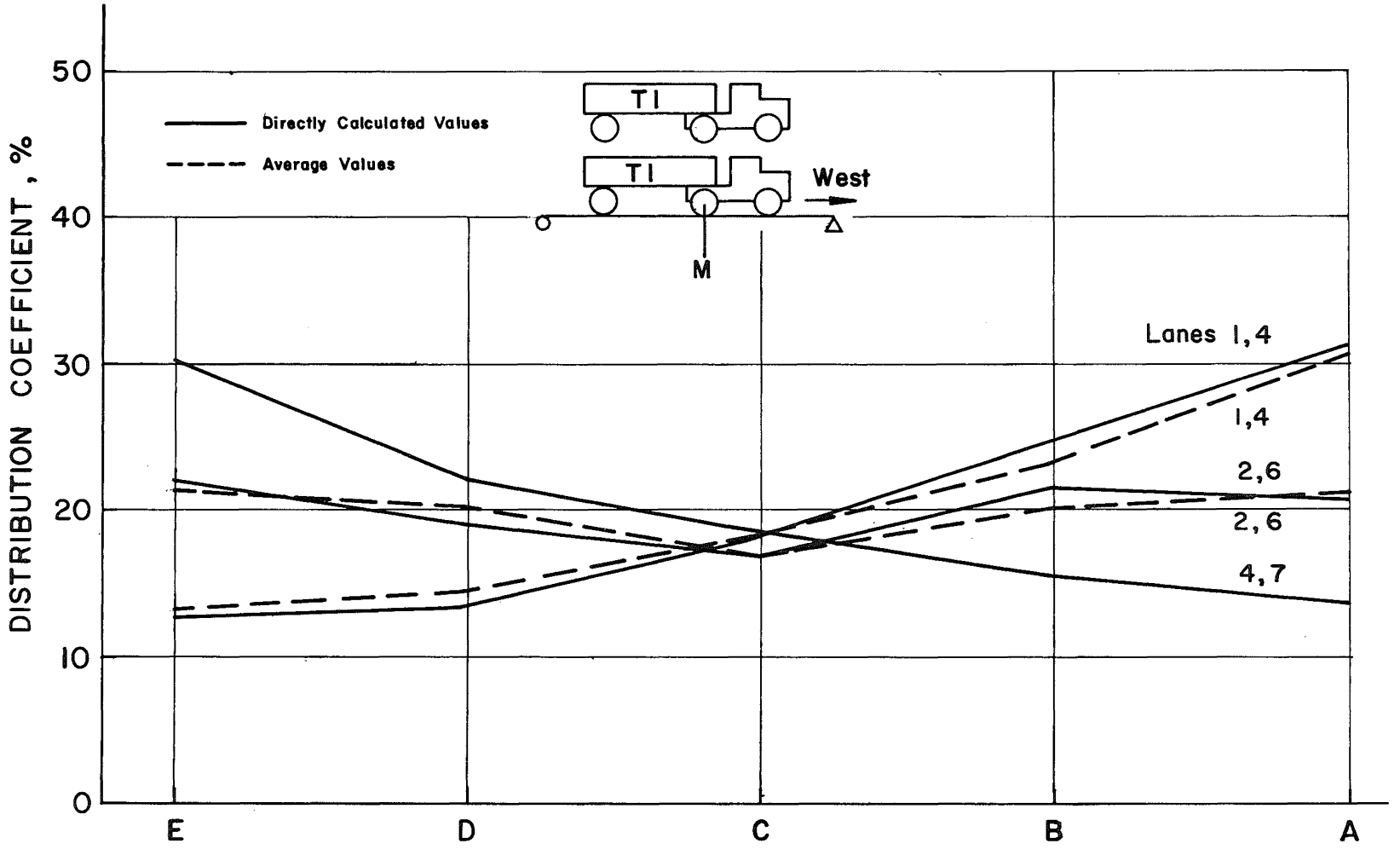

Fig. 31 Distribution Coefficients at Section M, Series II
(Superimposed Single-Truck Runs, T1 and T1, Westbound)

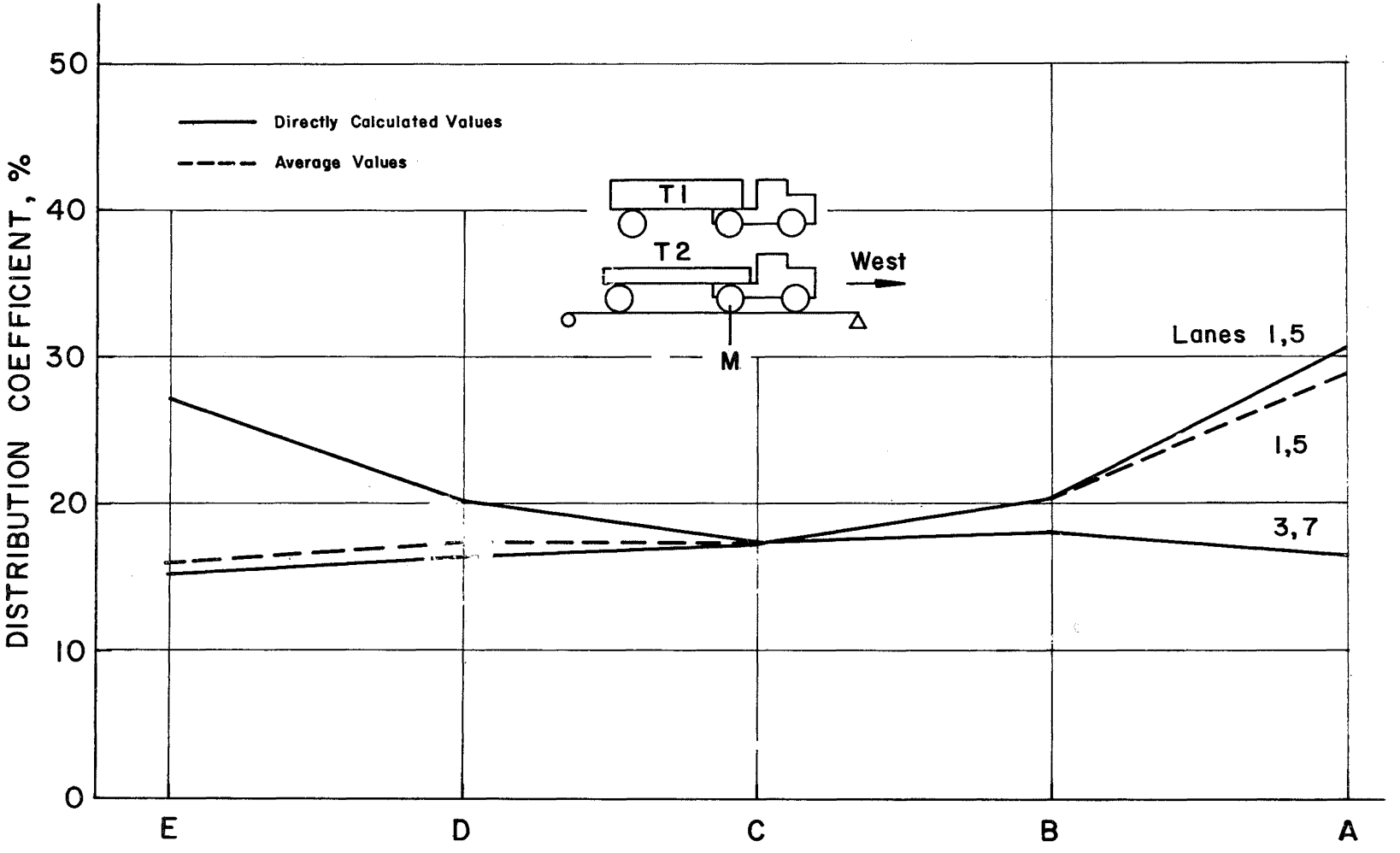

Fig. 32 Distribution Coefficients at Section M, Series II
(Superimposed Single-Truck Runs, T1 and T2, Westbound)
(AASHO Provisions for Lateral Truck Spacing)

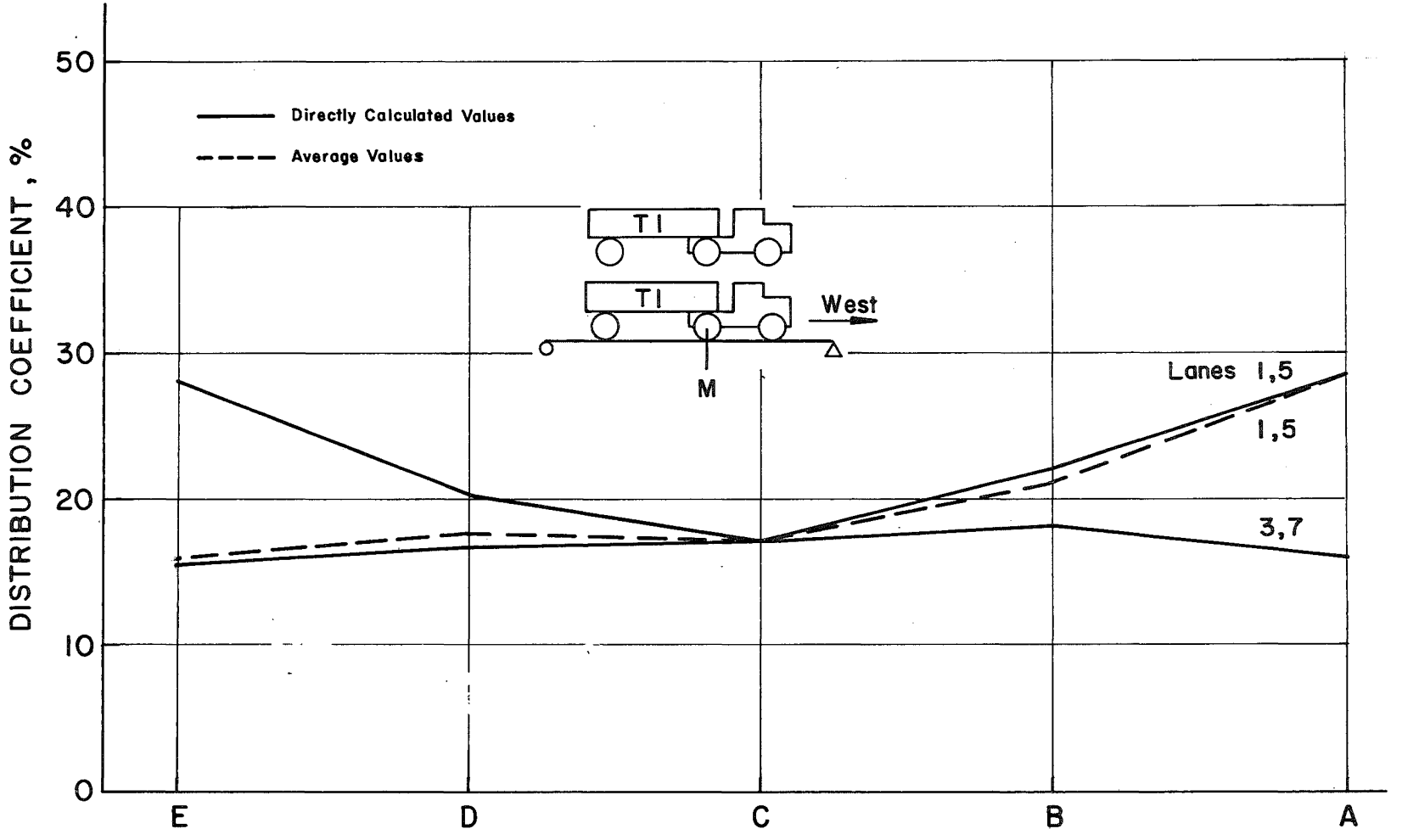

Fig. 33 Distribution Coefficients at Section M, Series II
(Superimposed Single-Truck Runs, T1 and T1, Westbound)
(AASHO Provisions for Lateral Truck Spacing)

10. REFERENCES

1. American Association of State Highway Officials
   STANDARD SPECIFICATIONS FOR HIGHWAY BRIDGES, Washington, D. C., 1961

2. American Concrete Institute
   ACI STANDARD BUILDING CODE REQUIREMENTS FOR REINFORCED CONCRETE, June 1963

3. Bouwkamp, J. G., Brown, C. B., Scheffey, C. F., and Yaghmai, S.
   BEHAVIOR OF A SINGLE SPAN COMPOSITE GIRDER BRIDGE, Structures and Materials Research, University of California, Berkeley, Department of Civil Engineering, Report SESM-65-5, August 1965

4. Davis, R. E., Kozak, J. J., and Scheffey, C. F.
   STRUCTURAL BEHAVIOR OF A CONCRETE BOX GIRDER BRIDGE, Highway Research Record, No. 76, Highway Research Board of the National Academy of Sciences - National Research Council, publication 1261, 1965

5. Foster, G. M.
   TEST ON ROLLED-BEAM BRIDGE USING H20-S16 LOADING, Distribution of Load Stresses in Highway Bridges, Highway Research Board Research Report 14-B, National Academy of Sciences - National Research Council, publication 253, January 1952

6. Hindman, W. S. and Vandegrift, L. E.
   LOAD DISTRIBUTION OVER CONTINUOUS DECK TYPE BRIDGE FLOOR SYSTEMS, Ohio State University, Engineering Experiment Station, Bulletin No. 122, XIV:No. 1, May 1945

7. Holcomb, R. M.
   DISTRIBUTION OF LOADS IN BEAM-AND-SLAB BRIDGES, Iowa State Highway Commission, Iowa Highway Research Board, Bulletin No. 12, December 1956

8. Hulsbos, C. L. and Linger, D. A.
   DYNAMIC TESTS OF A THREE-SPAN CONTINUOUS I-BEAM HIGHWAY BRIDGE, Iowa State University, Engineering Experiment Station, Report presented at the Highway Research Board Meeting, January 1960

9. Kinnier, H. L. and McKeel, W. T.
   A DYNAMIC STRESS STUDY OF THE HAZEL RIVER BRIDGE, Virginia Council of Highway Investigation and Research, Vibration Survey of Composite Bridges, Progress Report No. 3, September 1964

10. Linger, D. A. and Hulsbos, C. L.
DYNAMICS OF HIGHWAY BRIDGES, PART II STATIC AND DYNAMIC LOAD DISTRIBUTION, Iowa State Highway Commission, Iowa Highway Research Board, Bulletin No. 17, November 1960

11. Pennsylvania Department of Highways, Bridge Division
STANDARDS FOR PRESTRESSED CONCRETE BRIDGES, 1960

12. Prentzas, E. G.
DYNAMIC BEHAVIOR OF TWO CONTINUOUS I-BEAM BRIDGES, Iowa State Highway Commission, Iowa Highway Research Board, Bulletin No. 14, August 1958

13. Reilly, R., Guardia, G., and Looney, C. T. G.
DYNAMIC BEHAVIOR OF HIGHWAY BRIDGES: PROGRESS REPORT, TESTING AND DATA REDUCTION, University of Maryland, Civil Engineering Department, August 1964

14. Varney, R. F. and Galambos, C. F.
FIELD DYNAMIC LOADING STUDIES OF HIGHWAY BRIDGES IN THE U. S., 1948-1965, Highway Research Record, No. 76, Highway Research Board of the National Academy of Sciences - National Research Council, publication 1261, 1965

15. White, A. and Purnell, W. B.
LATERAL LOAD DISTRIBUTION ON I-BEAM BRIDGE, Journal of the Structural Division, Proceedings of the American Society of Civil Engineers, 83:ST3, Paper No. 1255, May 1957